UNIVERSIDAD NACIONAL AUTÓNOMA DE MÉXICO
POSGRADO EN CIENCIAS FÍSICAS
INSTITUTO DE CIENCIAS NUCLEARES

Neutral pion mass in a magnetized medium

Tesis

Que para optar por el grado de:
Maestro en Ciencias F´ısicas (F´
ısica)

Presenta:

José Luis Hernández Hernández

Tutor principal

José Alejandro Ayala Mercado
Instituto de Ciencias Nucleares, UNAM

Miembros del comité tutor

Wolfgang Peter Bietenholz
Instituto de Ciencias Nucleares, UNAM

Ángel Sánchez Cecilio
Facultad de Ciencias, UNAM

Ciudad de México, abril, 2021

Para mi madre

Agradecimientos

Expreso mi agradecimiento a todas las personas que hacen posible que la Universidad Nacional Autónoma de México (UNAM) sea un proyecto social de alto impacto en nuestro país. En la UNAM no solo recibí una excelente formación académica, la convivencia con diferentes personas y la experiencia que he adquirido a lo largo de estos años me han servido para ser consciente de la amplia variedad de problemas que afectan a nuestra sociedad y la necesidad de asumir el compromiso para solucionarlos.

Agradezco a mi padre Edilberto y a mi hermana Yuri por su apoyo durante estos años, a mi madre Gloria por siempre estar a mi lado y enseñarme a superar las adversidades con perseverancia y honestidad, y a los amigos que he tenido la oportunidad de conocer a lo largo del tiempo por su amistad y confianza.

El presente trabajo no hubiera sido posible sin las contribuciones de Alejandro Ayala, Luis Alberto Hernández, Ricardo Farias y Renato Zamora, con quienes he formado un excelente grupo de trabajo. En particular, a Alejandro y a Luis les doy gracias por el apoyo y los consejos que me han dado durante mis estudios y por motivarme a seguir aprendiendo. También expreso mi gratitud a los doctores Wolfgang Bietenholz, Ángel Sánchez, Norberto Scoccola y a la doctora Ana Júlia Mizher por sus observaciones que permitieron mejorar de forma significativa el contenido del escrito.

Finalmente, doy gracias al Consejo Nacional de Ciencia y Tecnología (CONACyT), al Instituto de Ciencias Nucleares, al Instituto de Física, al Programa de Apoyo a los Estudiantes de Posgrado (PAEP) y al Posgrado en Ciencias Físicas por el apoyo económico y administrativo proporcionado durante mis estudios de maestría.

Contents

Resumen

En este trabajo, se estudian los efectos de un campo magnético externo uniforme y constante sobre la masa del pión neutro en el contexto del modelo sigma lineal acoplado con quarks. La motivación principal de este estudio se fundamenta en la importancia de los efectos de un medio magnetizado sobre las propiedades básicas de los grados de libertad hadrónicos. Estas propiedades como funciones de la intensidad del campo magnético contribuyen a una descripción apropiada de sistemas físicos como estrellas de neutrones [1, 2] y el plasma de quarks y gluones generado en colisiones periféricas de iones pesados [3, 4].

Los piones neutros no experimentan directamente los efectos de un campo magnético y su masa a primera vista permanece intacta. Sin embargo, esta propiedad cambia una vez que se consideran las interacciones entre piones y otras partículas que se encuentran en el vacío fuertemente interactuante. A partir del origen dinámico de las masas de ciertas partículas, debido al rompimiento espontáneo de la simetría quiral, es posible estudiar sus modificaciones al considerar condiciones externas como lo son: la temperatura, densidad y campos electromagnéticos. Como consecuencia, las correcciones magnéticas a la masa del pión neutro han sido determinadas a través de diferentes técnicas. Los primeros cálculos que permitieron obtener las correcciones magnéticas a la masa del pión neutro corresponden al formalismo de la Cromodinámica Cuántica en la retícula ("*Lattice Quantum Chromodynamics*", LQCD, por sus siglas en inglés) [5,6], donde un comportamiento decreciente monótono de la masa como función de la intensidad de campo magnético es confirmado en la mayoría de los estudios realizados con dicho método. Otra técnica frecuentemente empleada es el uso de modelos efectivos. En el contexto de uno de ellos, el modelo sigma lineal acoplado con quarks, se ha determinado que la masa del pión neutro tiene un comportamiento decreciente en el régimen de campo débil [7]. Sin embargo, un estudio reciente en la Ref. [8], donde se incluyen las modificaciones magnéticas a los acoplamientos del modelo, predice que la masa comienza a decrecer y en un valor intermedio de la intensidad del campo magnético empieza a crecer superando su valor en ausencia de campo magnético. Estudios similares con el modelo de Nambu-Jona-Lasinio obtuvieron un comportamiento similar en la región de campo fuerte [9, 10].

En este trabajo, se busca responder si es posible reproducir el comportamiento decreciente obtenido por los resultados de LQCD a partir de un estudio en la aproximación de campo magnético intenso. Esta cuestión es abordada en un análisis que combina de manera apropiada una elección de parámetros libres en el modelo con el efecto del campo magnético externo a un lazo sobre los elementos involucrados en la relación de dispersión del pión neutro, a saber, el valor de expectación en el vacío del campo sigma, la autoenergía del pión neutro, el acoplamiento entre bosones y el acoplamiento bosón-fermión.

Siguiendo esta vía, las predicciones del modelo sigma lineal con quarks sujeto a un medio

magnetizado reproducen la dependencia de la intensidad del campo magnético en la masa del pión neutro reportada en los estudios recientes de LQCD, donde las técnicas utilizadas implementan valores de la masa del pión neutro en ausencia de campo magnético mayores al valor físico ($m_0 \approx 140$MeV). A través de una comparación de estos resultados, se obtuvo que cuando el valor físico de la masa del pión neutro en vacío es utilizado en nuestra aproximación, la curva que indica el comportamiento de la masa como función de la intensidad del campo está ligeramente por debajo de los datos obtenidos por LQCD. En este sentido, este resultado es nuestra predicción si en algún momento las técnicas de LQCD permiten realizar cálculos usando el valor físico de la masa del pión neutro. Además, mediante este estudio, fue posible mostrar un comportamiento creciente monótono para el valor de expectación en el vacío del campo sigma como función de la intensidad del campo magnético, dado que este valor en el modelo corresponde a un parámetro de orden, el comportamiento obtenido permite sustentar el fenómeno de catálisis magnética.

Finalmente, los resultados en este trabajo pueden ser utilizados para saber si mediante esta aproximación es posible reproducir el comportamiento de la masa de los piones cargados en presencia de un campo magnético externo con la misma elección de parámetros libres. Otros posibles escenarios donde los resultados de este trabajo pueden tener un impacto potencial incluyen el cálculo de la viscosidad laminar y de bulto en materia con quarks y mesones y la ecuación de estado nuclear en objetos astrofísicos densos y compactos, como lo son las estrellas de neutrones. Los resultados de esta investigación fueron reportados en las siguientes publicaciones [11, 12].

Chapter 1

Introduction

The study of quantum systems subject to electromagnetic fields has become an active area of research given the important role they play in quantum processes [13, 14]. In fact, it is well-known that several phenomena may arise in the presence of a classical electromagnetic field. A relevant example of this discussion is the breaking of chiral symmetry when we take into account an external magnetic field. Under such conditions, it has been demonstrated that a magnetized medium has a strong tendency to produce stronger quark-antiquark condensates, which are associated with the spontaneous chiral symmetry breaking. This mechanism seems to be universal and model-independent and it is referred to the literature as *magnetic catalysis* [15–17]. On the other hand, when temperature is considered, magnetic fields suppress the condensate formation producing the opposite effect whereby the pseudocritical temperature for the chiral phase transition is reduced, this is the so-called *inverse magnetic catalysis* [18–34].

Furthermore, much effort has also been invested to study the basic properties of magnetized hadronic degrees of freedom. The subject is relevant *e.g.* for a suitable description of physical systems such as cold neutron stars [1, 2] and the quark gluon plasma generated in heavy ion collisions [3, 4]. As is well known, the nuclear equation of state is affected by baryon and meson masses and couplings, this fact motivates studies intented to understand how these parameters change in the presence of electromagnetic fields [35–47].

Due to the dynamical origin of mass for certain particles through the chiral symmetry breaking, it is plausible to investigate the mass modifications by external conditions. As a starting point, because of their relevant role in the chiral symmetry breaking, it is important to study the magnetic field effects on pion properties such as masses and form factors.

On general grounds, charged and neutral pions behave differently under the influence of an external magnetic field. On one hand, charged pions with mass m_0 and at rest in the direction of the magnetic field, have an energy spectrum given by

$$E^2 = m_0^2 + (2n+1)|eB|, \tag{1.1}$$

where B is the field strength, e is the charge of the positron and n labels the n th Landau level. The lowest-energy state can be interpreted as the magnetic-field-dependent mass, which is then given by

$$m_B^2 = m_0^2 + |eB|. \tag{1.2}$$

On the other hand, neutral pions do not experience directly the effects of a magnetic field, and, thus, their mass remains at first sight unaffected. However, this property changes once

we consider the interactions between pions and other particles that populate the strongly interacting vacuum.

Actually, the magnetic-field-driven modifications of the neutral pion mass were first determined using lattice QCD (LQCD) calculations in Refs. [5, 6]. These works found contradictory results: Ref. [6] obtains a neutral pion mass that monotonically decreases with the field strength, whereas Ref. [5] finds a dip at an intermediate value and then an increase for larger field strengths. This discussion was revisited in Refs. [48, 49], where the monotonic decrease of the pion mass as a function of the field strength was confirmed.

Another approach involves the use of effective field theories. Working in the context of the linear sigma model with quarks (LSMq) in the weak field limit, Ref. [7] has shown that the neutral pions mass decreases as a function of the field strength in the weak field regime. In this study, the magnetic field modification of the boson self-coupling was highlighted as a key element in the behavior of the magnetic modification of the neutral pion mass. Recently, Ref. [8], using the same model and accounting for the magnetic-field-driven modifications of the couplings, found that the neutral pion mass begins to decrease and at an intermediate value it starts increasing to exceed the neutral pion mass in vacuum. A similar study in Refs. [9, 10] with the Nambu-Jona-Lasinio (NJL) model obtained the same behavior.

In this work we intent to answer whether the LSMq is able to reproduced the monotonically decreasing behavior of the recent LQCD results taking into account an analysis in the strong field regime. We address this question by means of an analysis which properly combines the setting of the free parameters of the model with the effects of the magnetic field corrections at one-loop order of the elements involved in the neutral pion mass dispersion relation, namely, the vacuum expectation value of the sigma field, the neutral pion self-energy, the boson self-coupling and boson-fermion coupling. The results of this project were reported in the following published articles [11, 12].

This work is organized as follows: In Chap. 2, the linear sigma model with quarks is introduced. Chapter 3 is devoted to discuss the field strength dependence of the propagators for the bosonic and fermionic cases in a constant uniform magnetic field. Chapter 4 contains the necessary elements to obtain the magnetic corrections to the pion mass at one-loop order. In Chap. 5, the neutral pion mass is calculated from its dispersion relation and compared with the recent LQCD calculations, showing in all cases that the monotonic decrease with the field strength can be reproduced for an appropriate choice of parameters. Conclusions and a brief summary are presented in Chap. 6. Finally, a brief discussion about the regularization and renormalization procedures, some useful dimensional regularization formulas and the explicit computation of the one-loop corrections to the effective potential, the self-energy and the couplings are shown in the appendixes.

Chapter 2

The linear sigma model coupled with quarks

In this chapter the LSMq is introduced as an effective field theory of QCD in the low-energy regime, the chiral symmetry in this model and the spontaneous symmetry breaking (SSB) are discussed. Finally, a list of the Feynman rules of this theory is presented.

The LSMq was introduced in 1960s by Gell-Mann and Lévy as a model to describe the pion-nucleon interaction [50]. This model can be adapted to describe the interactions among small-mass mesons and quarks and captures the approximate chiral symmetry of two-flavor QCD. The Lagrangian of the LSMq with two species of massless quarks u and d is given by

$$\mathcal{L} = \frac{1}{2}(\partial_\mu\sigma)^2 + \frac{1}{2}(\partial_\mu\vec{\pi})^2 + \frac{a^2}{2}(\sigma^2+\vec{\pi}^2) - \frac{\lambda}{4}(\sigma^2+\vec{\pi}^2)^2 + i\bar{\psi}\gamma^\mu\partial_\mu\psi - ig\gamma^5\bar{\psi}\vec{\tau}\cdot\vec{\pi}\psi - g\bar{\psi}\psi\sigma, \quad (2.1)$$

where $\vec{\tau} = (\tau_1, \tau_2, \tau_3)$ are the Pauli matrices,

$$\psi_{L,R} = \begin{pmatrix} u \\ d \end{pmatrix}_{L,R}, \quad (2.2)$$

is a $SU(2)_{L,R}$ doublet, σ is a real scalar field and $\vec{\pi} = (\pi_1, \pi_2, \pi_3)$ is a triplet of real scalar fields. π_3 corresponds to the neutral pion, whereas the charged ones are represented by the combinations

$$\pi_- = \frac{1}{\sqrt{2}}(\pi_1 + i\pi_2), \quad \pi_+ = \frac{1}{\sqrt{2}}(\pi_1 - i\pi_2). \quad (2.3)$$

λ is the boson's self-coupling and g is the fermion-boson coupling. $a^2 > 0$ is the mass squared parameter. Eq. (2.1) can be written in terms of the charged and neutral-pion degrees of freedom as

$$\begin{aligned}\mathcal{L} &= \frac{1}{2}[(\partial_\mu\sigma)^2 + (\partial_\mu\pi_0)^2] + \partial_\mu\pi_-\partial^\mu\pi_+ + \frac{a^2}{2}(\sigma^2+\pi_0^2) + a^2\pi_-\pi_+ - \frac{\lambda}{4}(\sigma^4 + 4\pi_-^2\pi_+^2 + 2\sigma^2\pi_0^2 \\ &+ 4\sigma^2\pi_-\pi_+ + 4\pi_-\pi_+\pi_0^2 + \pi_0^4) + i\bar{\psi}\partial\!\!\!/\psi - g\bar{\psi}\psi\sigma - ig\gamma^5\bar{\psi}(\tau_+\pi_+ + \tau_-\pi_- + \tau_3\pi_0)\psi, \quad (2.4)\end{aligned}$$

where the combination of Pauli matrices are defined as follows

$$\tau_+ = \frac{1}{\sqrt{2}}(\tau_1 + i\tau_2), \quad \tau_- = \frac{1}{\sqrt{2}}(\tau_1 - i\tau_2). \quad (2.5)$$

The LSMq Lagrangian is invariant under $SU(2)_L \times SU(2)_R$ chiral transformation [51]

$$\psi_{L,R} \to \exp(-i\vec{\theta}_{L,R} \cdot \vec{\tau})\psi_{L,R}. \tag{2.6}$$

However, the chiral symmetry does not appear in the low-energy particle spectrum since it is spontaneously broken.

2.1 SSB of chiral symmetry in the linear sigma model with quarks

Since chiral symmetry is spontaneously broken, the σ field acquires a non-vanishing vacuum expectation value

$$\sigma \to \sigma + v,$$

which breaks the $SU(2)_L \times SU(2)_R$ symmetry down to $SU(2)_{L+R}$. Moreover, v is an order parameter in this model: when this shift goes to zero the chiral symmetry is restored. Once the order parameter is considered explicitly, the resulting Lagrangian can be expressed as follows

$$\begin{aligned} \mathcal{L} &= \frac{1}{2}\partial_\mu\sigma\partial^\mu\sigma + \frac{1}{2}\partial_\mu\pi_0\partial^\mu\pi_0 + \partial_\mu\pi_-\partial^\mu\pi_+ - \frac{1}{2}m_\sigma^2(v)\sigma^2 - \frac{1}{2}m_0^2(v)\pi_0^2 \\ &- m_0^2(v)\pi_-\pi_+ + i\bar{\psi}\partial\!\!\!/\psi - m_f(v)\bar{\psi}\psi + \mathcal{L}_{int} - V_{tree}, \end{aligned} \tag{2.7}$$

where the interaction Lagrangian is defined as

$$\begin{aligned} \mathcal{L}_{int} &= -\frac{\lambda}{4}\sigma^4 - \lambda v\sigma^3 - \lambda v^3\sigma - \lambda\sigma^2\pi_-\pi_+ - 2\lambda v\sigma\pi_-\pi_+ - \frac{\lambda}{2}\sigma^2\pi_0^2 - \lambda v\sigma\pi_0^2 - \lambda\pi_-^2\pi_+^2 \\ &- \lambda\pi_-\pi_+\pi_0^2 - \frac{\lambda}{4}\pi_0^4 + a^2 v\sigma - g\bar{\psi}\psi\sigma - ig\gamma^5\bar{\psi}\left(\tau_+\pi_+ + \tau_-\pi_- + \tau_3\pi_0\right)\psi, \end{aligned} \tag{2.8}$$

and the fields develop masses given by

$$m_\sigma^2(v) = 3\lambda v^2 - a^2, \quad m_0^2(v) = \lambda v^2 - a^2, \quad m_f(v) = gv. \tag{2.9}$$

Doing explicitly the matrix product in the flavour space, the interaction Lagrangian can be written as

$$\begin{aligned} \mathcal{L}_{int} &= -\frac{\lambda}{4}\sigma^4 - \lambda v\sigma^3 - \lambda v^3\sigma - \lambda\sigma^2\pi_-\pi_+ - 2\lambda v\sigma\pi_-\pi_+ - \frac{\lambda}{2}\sigma^2\pi_0^2 - \lambda v\sigma\pi_0^2 - \lambda\pi_-^2\pi_+^2 - \frac{\lambda}{4}\pi_0^4 \\ &- \lambda\pi_-\pi_+\pi_0^2 - i\sqrt{2}g\left(\bar{u}\gamma^5 d\pi_+ + \bar{d}\gamma^5 u\pi_-\right) - ig\bar{u}\gamma^5 u\pi_0 + ig\bar{d}\gamma^5 d\pi_0 - g\bar{u}u\sigma - g\bar{d}d\sigma. \end{aligned} \tag{2.10}$$

Furthermore, the tree-level potential is given by

$$V_{tree} = -\frac{a^2}{2}v^2 + \frac{\lambda}{4}v^4, \tag{2.11}$$

this expression has a minimum as a function of v, called the vacuum expectation value of the σ field, namely,

$$v_0 = \sqrt{\frac{a^2}{\lambda}}. \tag{2.12}$$

As a consequence of the spontaneous symmetry breaking, three massless Goldstone bosons are generated, namely, the neutral and charged pions. In fact, when $v = v_0$, the linear term in σ vanishes and the pions become massless. However, the σ and quark fields remain massive, unlike in the case of QCD with massless dynamical quarks.

In order to include a finite pion mass, m_0 (fixed value, independent of v), one adds an explicit symmetry-breaking term [51] in the Lagrangian of Eq. (2.7) such that

$$\mathcal{L} \to \mathcal{L}' = \mathcal{L} + \frac{m_0^2}{2} v(\sigma + v). \tag{2.13}$$

This term modifies the tree-level potential. In particular, the minimum is shifted according to the following expression

$$v_0 \to v_0' = \sqrt{\frac{a^2 + m_0^2}{\lambda}}. \tag{2.14}$$

Correspondingly, the expressions for the masses, evaluated at the minimum obtained after the explicit breaking of the symmetry, are given by

$$\begin{aligned} m_f(v_0') &= g\sqrt{\frac{a^2 + m_0^2}{\lambda}}, \\ m_\sigma^2(v_0') &= 2a^2 + 3m_0^2, \\ m_0^2(v_0') &= m_0^2. \end{aligned} \tag{2.15}$$

Furthermore, from Eq. (2.15), we can get an expression for the parameter a, which is given by

$$a = \sqrt{\frac{m_\sigma^2 - 3m_0^2}{2}}. \tag{2.16}$$

Setting $m_0 = 140$ MeV and $m_\sigma = 400 - 600$ MeV, we get $a = 225 - 390$ MeV.

2.2 Feynman rules of the linear sigma model with quarks

This chapter concludes by listing the Feynman rules deduced from the Lagrangian density in Eq. (2.10). After accounting for the number of permutations for a set of equivalent lines and a factor of i coming from the action, these are displayed in Fig. 2.1 and Fig. 2.2. Fig. 2.1 shows the vertices arising in the meson sector and Fig. 2.2 shows the quark-meson vertices. Dashed lines represent the neutral and charged pions and double lines represent the σ, whereas thin solid lines represent the d quark and thick solid lines represent the u quark.

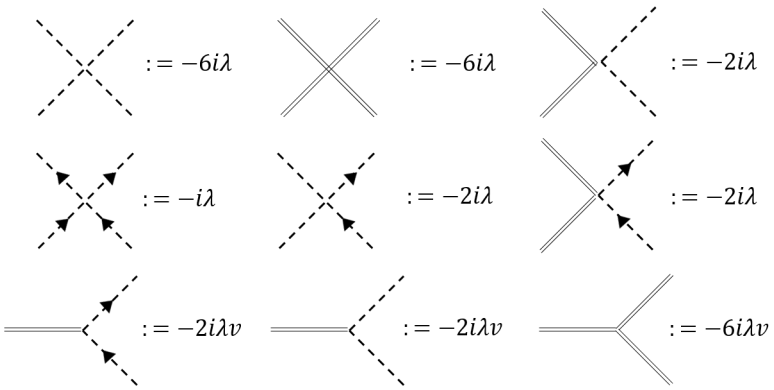

Figure 2.1: Meson interactions in the LSMq. Dashed lines are used to represent the neutral and charged pions, whereas double lines represent the σ.

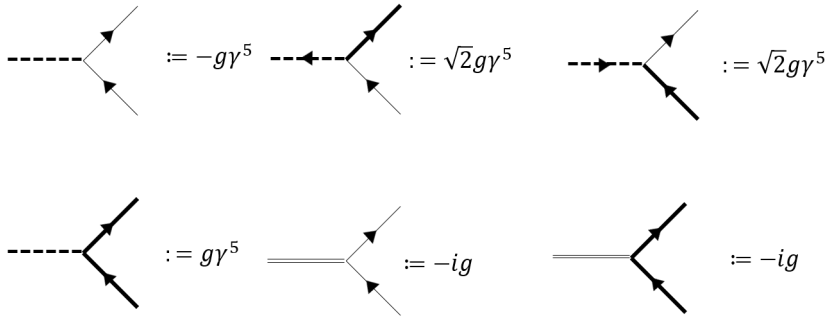

Figure 2.2: Quark-meson interactions in the LSMq. Dashed lines represent the neutral and charged pions, whereas the double lines represent the σ. Solid lines represent the quarks. Thin solid lines represent the d quark and thick solid lines represent the u quark.

Up to this point, we have the neccessary elements to study the LSMq from a perturbative approach. The process to include the effects from a uniform constant magnetic field is described in the next chapter.

Chapter 3

Classical magnetic field in QFT

This chapter is devoted to briefly discussing the way we include the effect of an external magnetic field in the LSMq and some representations for the propagators of charged particles subject to a constant uniform magnetic field.

With the purpose of considering the effects of a magnetized medium in the propagation of the charged modes, we make the minimal substitution in the Lagrangian of Eq.(2.7)

$$\partial_\mu \to D_\mu = \partial_\mu + iqA_\mu, \tag{3.1}$$

where q is the particle's electric charge and A_μ is the vector potential. Choosing the magnetic field to point in the direction of the $\hat{z}$ axis, namely, $\vec{B} = B\hat{z}$, the vector potential can be expressed in the symmetric gauge as

$$A^\mu(x) = \frac{1}{2}x_\nu F^{\nu\mu}. \tag{3.2}$$

A gauge transformation can be perfomed in the vector potential as

$$A^\mu(x) \to A'^\mu(x) = A^\mu(x) + \partial^\mu\Lambda(x), \tag{3.3}$$

where Λ is a well-behaved function determined by the gauge choice. As a consequence, a more general expression can be written as a gauge transformation from the symmetric gauge to an arbitrary gauge:

$$A^\mu(x) = \frac{1}{2}x_\nu F^{\nu\mu} + \partial^\mu\Lambda(x). \tag{3.4}$$

3.1 Propagators of charged particles

Notice that the ordinary derivative becomes the covariant derivative only for particles with non-vanishing electric charge. As a consequence, the propagation of charged bosons and fermions is described by propagators in the presence of a constant magnetic field. Using the Schwinger proper time representation [52], the fermion propagator can be written as

$$S(x, x') = e^{i\Phi(x,x')}S(x - x'), \tag{3.5}$$

where $\Phi(x, x')$ is the Schwinger phase given by

$$\Phi(x, x') = q\int_x^{x'} d\xi_\mu \left[A^\mu(\xi) + \frac{1}{2}F^{\mu\nu}(\xi - x')_\nu\right], \tag{3.6}$$

and represents the translationally noninvariant and gauge-dependent part of the propagator in the presence of a magnetic background. Using Eq.(3.4) with Eq.(3.6), the Schwinger phase can be computed using the expression [14]

$$\Phi(x,x') = q\left[\frac{1}{2}x^{\mu}F_{\mu\nu}x'^{\nu} + \Lambda(x') - \Lambda(x)\right], \tag{3.7}$$

On the other hand, $S(x-x')$ is translationally and gauge invariant and can be expressed in terms of its Fourier transform as

$$S(x-x') = \int \frac{d^4p}{(2\pi)^4} S(p) e^{-ip\cdot(x-x')}, \tag{3.8}$$

where

$$\begin{aligned} iS(p) &= \int_0^\infty \frac{ds}{\cos(|qB|s)} e^{is\left(p_\parallel^2 - p_\perp^2 \frac{\tan(|qB|s)}{|qB|s} - m_f^2 + i\epsilon\right)} \left[\left(m_f + \not{p}_\parallel\right)\left(\cos(|qB|s)\right.\right. \\ &+ \left.\left.\gamma^1\gamma^2 \sin(|qB|s)\mathrm{sgn}(qB)\right) - \frac{\not{p}_\perp}{\cos(|qB|s)}\right]. \end{aligned} \tag{3.9}$$

Hereafter γ^0, γ^1, γ^2, γ^3 and $\gamma^5 = i\gamma^0\gamma^1\gamma^2\gamma^3$ are Dirac matrices. The four-vectors with the indexes $\perp$ and $\parallel$ belong to the Euclidean $\{1,2\}$-subspace and the Minkowski $\{0,3\}$-subspace respectively [53]. As a consequence, $a_\parallel \cdot b_\parallel = a_0 b_0 - a_3 b_3$ and $a_\perp \cdot b_\perp = a_1 b_1 + a_2 b_2$ where $a_\parallel^\mu = (a_0, 0, 0, a_3)$, $b_\parallel^\mu = (b_0, 0, 0, b_3)$, $a_\perp^\mu = (0, a_1, a_2, 0)$ and $b_\perp^\mu = (0, b_1, b_2, 0)$. Accordingly, the Feynman slash notation is used, $\not{a}_\parallel = a_\parallel^\mu \gamma_\mu$ and $\not{a}_\perp = a_\perp^\mu \gamma_\mu$.

In a similar fashion, for a charged scalar field, we have

$$D(x,x') = e^{i\Phi(x,x')} D(x-x'), \tag{3.10}$$

where the translationally and gauge-invariant part of the propagator is given by

$$D(x-x') = \int \frac{d^4p}{(2\pi)^4} D(p) e^{-ip\cdot(x-x')}, \tag{3.11}$$

with

$$iD(p) = \int_0^\infty \frac{ds}{\cos(|qB|s)} e^{is\left(p_\parallel^2 - p_\perp^2 \frac{\tan(|qB|s)}{|qB|s} - m_b^2 + i\epsilon\right)}, \tag{3.12}$$

where the boson and fermion masses are m_b and m_f, respectively. It is worth to mention that the integration over the proper time, s, in Eqs.(3.9), (3.12) is performed in a complex plane s over the contour that begins in the point $s = 0$ and lies below the real axis due to the poles of the integrand [53].

3.2 Expansion over Landau levels

The propagators in Eqs. (3.9) and (3.12) can also be expanded as a sum over Landau levels [13, 53, 54]. In this last representation, the expressions for the charged scalar and a fermion propagators are given by

$$iD(p) = 2ie^{-\frac{p_\perp^2}{|qB|}} \sum_{n=0}^{\infty} \frac{(-1)^n L_n^0\left(\frac{2p_\perp^2}{|qB|}\right)}{p_\parallel^2 - m_b^2 - (2n+1)|qB| + i\epsilon}, \tag{3.13}$$

$$iS(p) = ie^{-\frac{p_\perp^2}{|qB|}} \sum_{n=0}^{\infty} \frac{(-1)^n D_n(p)}{p_\parallel^2 - m_f^2 - 2n|qB| + i\epsilon}, \tag{3.14}$$

where

$$D_n(p) = 2(\not{p}_\parallel + m_f)\mathcal{O}^+ L_n^0\left(\frac{2p_\perp^2}{|qB|}\right) - 2(\not{p}_\parallel + m_f)\mathcal{O}^- L_{n-1}^0\left(\frac{2p_\perp^2}{|qB|}\right) + 4\not{p}_\perp L_{n-1}^1\left(\frac{2p_\perp^2}{|qB|}\right), \tag{3.15}$$

respectively; $L_n^m(x)$ are the generalized Laguerre polynomials and $L_{-1}^0(x) = 0$. In Eq. (3.15) the projection operators $\mathcal{O}^\pm$ are defined as

$$\mathcal{O}^\pm = \frac{1}{2}\left(1 \pm i\gamma_1\gamma_2\,\mathrm{sign}(qB)\right). \tag{3.16}$$

3.3 Strong magnetic field approximation

In the strong field limit, if charged particles do not have enough momentum to overcome the energy gap between succesive energy levels or Landau levels, one can consider the lowest Landau level (LLL) as a good aproximation for this physical situation. On one hand, considering just the contribution from $n = 0$ in Eqs. (3.14) and (3.15), we have

$$iS \to iS^{LLL}(k) = 2ie^{\frac{-k_\perp^2}{|qB|}} \frac{\not{k}_\parallel + m_f}{k_\parallel^2 - m_f^2 + i\epsilon}\mathcal{O}^+, \tag{3.17}$$

where the projection operator $\mathcal{O}^+$ reflects the spin polarized nature of the ground state, the orientation of the spin is parallel (antiparallel) to the magnetic field in the case of a positive (negative) electric charge of the fermions [13].

On the other hand, the propagator of a charge scalar particle in the Lowest Landau Level approximation is given by the following equation

$$iD \to iD^{LLL}(k) = \frac{2ie^{-\frac{k_\perp^2}{|qB|}}}{k_\parallel^2 - m_b^2 - |qB| + i\epsilon}. \tag{3.18}$$

In both Eqs.(3.17) and (3.18) the transverse and longitudinal momenta decouple.

With these expressions at hand, we are able to perform calculations at one-loop order considering the effects from a uniform constant magnetic field.

Chapter 4

One-loop magnetic corrections

The necessary elements to determine the magnetic corrections to the neutral pion mass at one-loop are discussed in detail in this section. The starting point to compute the magnetic-field-induced modification to the neutral pion mass is the equation defining its dispersion relation in the presence of the magnetic field, namely,

$$q_0^2 - |\vec{q}|^2 - m_0^2(\lambda_B, v_B) - \mathrm{Re}[\Pi(B, q; \lambda_B, g_B, v_B)] = 0, \tag{4.1}$$

where Π is the neutral pion self-energy, and λ_B, g_B, v_B represent the magnetic-field-dependent boson-self coupling, boson-fermion coupling and vacuum expectation value, respectively. The computation requires knowledge of each of these elements as functions of the field strength. v_B can be computed finding the minimum of the magnetic-field-dependent one-loop effective potential. This can be analytically computed using the full magnetic field dependence of the charged particle propagators. For the neutral pion self-energy and the magnetic field corrections to the couplings, we work in the large field limit and, thus, resort to using propagators in the LLL approximation.

4.1 Magnetic corrections to the vacuum expectation value

The magnetic correction to the vacuum expectation value can be obtained by identifying the minimum for the effective potential in the presence of the magnetic background, v_B. For the LSMq in a magnetized medium, the effective potential at one-loop contains fermion as well as boson contributions which modify the location of the minimum as a function of the field strength. The effective potential up to one-loop order has six contributions, namely,

$$V^{eff} = V^{tree} + V^1_{\pi^0} + V^1_{\sigma} + V^1_{\pi^-} + V^1_{\pi^+} + \sum_f V^1_f. \tag{4.2}$$

The first term on the right-hand side of Eq. (4.2) represents the classical or tree-level potential and it can be read off from Eqs. (2.7) and (2.11). The second and third terms are the neutral contributions associated with the sigma and neutral pion, respectively. The remaining terms include the magnetic modifications to the effective potential, the fourth and fifth terms are associated with the charged pions, while the last one is the fermion contribution. To

illustrate the computation of these corrections at one-loop order, we study the general case for the bosonic and fermionic contributions to the effective potential.

First, the contribution to the effective potential at one-loop from a charged boson with mass m_b and charge q_b is given by the expression [55]

$$V_b^1 = -\frac{i}{2}\int \frac{d^4k}{(2\pi)^4}\ln\left[-D_b^{-1}(k)\right], \tag{4.3}$$

where the charged boson propagator is given by Eq. (3.13). The computation of Eq. (4.3) is performed in Appendix B. In fact, an analytical expression for an arbitrary magnetic field strength can be found. Working in the $\overline{\text{MS}}$ renormalization scheme this expression is given by

$$V_b^1 = \frac{1}{16\pi^2}\left[2|q_bB|^2\psi^{-2}\left(\frac{1}{2}+\frac{m_b^2}{2|q_bB|}\right)-\frac{1}{2}|q_bB|m_b^2\ln(2\pi)-\frac{m_b^4}{4}\ln\left(\frac{\mu^2}{m_b^2}\right)-\frac{m_b^4}{4}\ln\left(\frac{m_b^2}{2|q_bB|}\right)\right], \tag{4.4}$$

where $\psi^{-2}(x)$ is the polygamma function of the order of -2 and μ is the renormalization scale. Notice that in the limit $B\to 0$, Eq. (4.4) becomes

$$V_b^1 \xrightarrow[B\to 0]{} V_b^1 = -\frac{m_b^4}{64\pi^2}\left[\frac{3}{2}+\ln\left(\frac{\mu^2}{m_b^2}\right)\right], \tag{4.5}$$

which corresponds to the contribution to the effective potential from a neutral boson with mass m_b [56]. Thus, we use Eq. (4.5) to account for the contribution coming from the fourth and fifth terms of Eq. (4.2). In order to identify the purely magnetic contribution from Eq. (4.4), $V_{b(B)}^1$, we subtract Eq. (4.5) from Eq. (4.4) such as

$$V_{b(B)}^1 = \frac{1}{16\pi^2}\left[2|eB|^2\psi^{-2}\left(\frac{1}{2}+\frac{m_b^2}{2|eB|}\right)-\frac{1}{2}|eB|m_b^2\ln(2\pi)-\frac{m_b^4}{4}\ln\left(\frac{m_b^2}{2|eB|}\right)+\frac{3m_b^4}{8}\right]. \tag{4.6}$$

In the second place, the contribution from a single fermion with mass m_f and charge q_f can be obtained from the expression [57]

$$V_f^1 = iN_c\int\frac{d^4k}{(2\pi)^4}\text{Tr}\left[\ln\left(S_f^{-1}(k)\right)\right], \tag{4.7}$$

where N_c is the number of colors and $iS_f(k)$ is given by Eqs. (3.14) and (3.15). The explicit computation is shown in Appendix B. Once again, the result can be provided for an arbitrary field strength. Working with the $\overline{\text{MS}}$ renormalization scheme, this is given by

$$V_f^1 = -\frac{N_c}{8\pi^2}\left(4|q_fB|^2\psi^{-2}\left(\frac{m_f^2}{2|q_fB|}\right)-\frac{m_f^4}{2}\ln\left(\frac{\mu^2}{2|q_fB|}\right)-m_f^2|q_fB|\left[1-\ln\left(\frac{m_f^2}{4\pi|q_fB|}\right)\right]\right). \tag{4.8}$$

In the limit $B\to 0$, Eq. (4.8) becomes

$$V_f^1 = N_c\frac{m_f^4}{16\pi^2}\left[\frac{3}{2}+\ln\left(\frac{\mu^2}{m_f^2}\right)\right], \tag{4.9}$$

which corresponds to the contribution to the effective potential from a fermion in the absence of the magnetic field. Thus, the purely magnetic contribution from Eq. (4.8) is given by

$$\begin{aligned} V^1_{f(B)} &= -\frac{N_c}{8\pi^2}\left[4|q_fB|^2\psi^{-2}\left(\frac{m_f^2}{2|q_fB|}\right) - \frac{m_f^4}{2}\ln\left(\frac{m_f^2}{2|q_fB|}\right) + \frac{3}{4}m_f^4 - m_f^2|q_fB|\right. \\ &+ \left. m_f^2|q_fB|\ln\left(\frac{m_f^2}{4\pi|q_fB|}\right)\right]. \end{aligned} \tag{4.10}$$

When the tree-level effective potential is modified by one-loop corrections, the curvature and the position of the minimum are bound to change, therefore the minimum becomes unstable under radiative corrections. The changes are driven both from purely vacuum contributions as well as from magnetic field effects. The vacuum modifications need to be absorbed with a redefinition of the vacuum terms so as to make sure that any change in the position of the minimum truly comes from the magnetized background. This is accomplished by enforcing the *vacuum stability conditions* [57, 58], introducing counterterms in such a way that

$$V^{\rm tree} \to V^{\rm tree} + \delta V^{\rm tree} = -\frac{a^2 + m_0^2 + \delta a^2}{2}v^2 + \frac{\lambda + \delta\lambda}{4}v^4, \tag{4.11}$$

where δa^2 and $\delta\lambda$ are to be determined from the conditions

$$\begin{aligned} \frac{1}{2v}\frac{dV^{\rm vac}}{dv}\bigg|_{v=v_0} &= 0, \\ \frac{d^2V^{\rm vac}}{dv^2}\bigg|_{v=v_0} &= 2a^2 + 2m_0^2. \end{aligned} \tag{4.12}$$

$V^{\rm vac}$ contains the contribution from the three pions, the σ and the three color charges for the two light quarks, in the limit $B \to 0$, namely,

$$\begin{aligned} V^{\rm vac} &= -\frac{a^2 + m_0^2 + \delta a^2}{2}v^2 + \frac{\lambda + \delta\lambda}{4}v^4 - 3\frac{m_0^4(v)}{64\pi^2}\left[\frac{3}{2} + \ln\left(\frac{\mu^2}{m_0^2(v)}\right)\right] \\ &- \frac{m_\sigma^4(v)}{64\pi^2}\left[\frac{3}{2} + \ln\left(\frac{\mu^2}{m_\sigma^2(v)}\right)\right] + 2N_c\sum_f \frac{m_f^4(v)}{16\pi^2}\left[\frac{3}{2} + \ln\left(\frac{\mu^2}{m_f^2(v)}\right)\right], \end{aligned} \tag{4.13}$$

where

$$\begin{aligned} \delta a^2 &= \frac{1}{16\pi^2\lambda}\left[8a^2g^4N_c + 8g^4m_0^2N_c - 6a^2\lambda^2 - 12m_0^2\lambda^2\right. \\ &+ \left. 3a^2\lambda^2\ln\left(\frac{\mu^2}{m_0^2}\right) + 3a^2\lambda^2\ln\left(\frac{\mu^2}{2a^2 + 3m_0^2}\right)\right], \end{aligned} \tag{4.14}$$

$$\delta\lambda = \frac{1}{16\pi^2}\left[3\lambda^2\ln\left(\frac{\mu^2}{m_0^2}\right) + 9\lambda^2\ln\left(\frac{\mu^2}{2a^2 + 3m_0^2}\right) - 8g^4N_c\ln\left(\frac{\lambda\mu^2}{g^2(a^2 + m_0^2)}\right)\right]. \tag{4.15}$$

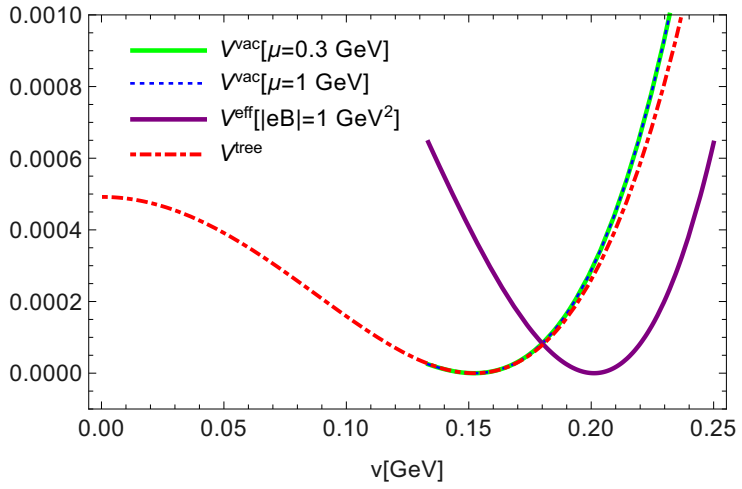

Figure 4.1: Comparison between the position and curvature of the minimum of $V^{\rm tree}$ and $V^{\rm vac}$ computed with $\mu = 0.3$ GeV and 1 GeV, after implementing the vacuum stability conditions. Also, an example of the position of the minimum for $V^{\rm eff}$, v_B, computed with $|eB| = 1$ GeV^2 is shown. For the calculation we use $m_0 = 140$ MeV, $\lambda = 3.67$, $g = 0.46$, and, correspondingly, $m_\sigma = 435$ MeV, $a = 256$ MeV, and $v_0 = 152$ MeV.

Therefore, once we include the vacuum terms evaluated on the vacuum expectation value in the effective potential at finite magnetic field and set the stability conditions to suppress the vacuum corrections, we accomplish that the modifications to the minimum come from the purely magnetic effects, namely, the charged pions and fermions contributions. As a result, the one-loop effective potential in a magnetized medium can be written as

$$\begin{aligned} V^{eff}(B) &= -\frac{a^2+m_0^2}{2}v^2 - \frac{\delta a^2}{2}v_0^2 + \frac{\lambda}{4}v^4 + \frac{\delta\lambda}{4}v_0^4 - 3\frac{m_0^4(v_0)}{64\pi^2}\left[\frac{3}{2} + \ln\left(\frac{\mu^2}{m_0^2(v_0)}\right)\right] \\ &- \frac{m_\sigma^4(v_0)}{64\pi^2}\left[\frac{3}{2} + \ln\left(\frac{\mu^2}{m_\sigma^2(v_0)}\right)\right] + 2N_c\sum_f \frac{m_f^4(v_0)}{16\pi^2}\left[\frac{3}{2} + \ln\left(\frac{\mu^2}{m_f^2(v_0)}\right)\right] \\ &+ \frac{2}{16\pi^2}\left[2|eB|^2\,\psi^{-2}\left(\frac{1}{2} + \frac{m_0^2(v)}{2|eB|}\right) - \frac{1}{2}|eB|\,m_0^2(v)\ln(2\pi) - \frac{m_0^4(v)}{4}\ln\left(\frac{m_0^2(v)}{2|eB|}\right)\right. \\ &+ \left.\frac{3m_0^4(v)}{8}\right] - \frac{N_c}{8\pi^2}\sum_f\left[4|q_fB|^2\psi^{-2}\left(\frac{m_f^2(v)}{2|q_fB|}\right) - \frac{m_f^4(v)}{2}\ln\left(\frac{m_f^2(v)}{2|q_fB|}\right) + \frac{3}{4}m_f^4(v)\right. \\ &- \left. m_f^2(v)|q_fB| + m_f^2(v)|q_fB|\ln\left(\frac{m_f^2(v)}{4\pi|q_fB|}\right)\right]. \end{aligned} \tag{4.16}$$

Up to this point, we use natural units so that the speed of light, c, and the reduced Planck constant, $\hbar$, become: $c = \hbar = 1$. According to these constraints, the units of electrical charge, also, can be redefined by choosing $\varepsilon_0 = 1$ where ε_0 is the vacuum permittivity. Since

$$c^2 = \frac{1}{\varepsilon_0\mu_0}, \tag{4.17}$$

the vacuum permeability, μ_0, equals to 1. The value of the fine structure constant, α_{em}, is a dimentionless quantity with the same value in all systems of units. In natural units, α_{em}

becomes

$$\alpha_{em} = \frac{e^2}{4\pi} \approx \frac{1}{137}. \tag{4.18}$$

This clearly shows that the elementary electric charge has no dimensions in this system and $e \approx 0.303$.

Fig. 4.1 shows the tree-level potential V^{tree} and the vacuum one-loop potential V^{vac} computed for $\mu = 0.3$ GeV and 1 GeV, after implementing the stability conditions. Notice that after the vacuum stability conditions are implemented, the vacuum position and curvature remain at their tree-level values and that these quantities are independent of the choice of the renormalization scale μ. Also, shown in the figure is the magnetic-field-modified position of the minimum when adding the magnetic effects to the tree-level potential, for $|eB| = 1$ GeV^2. Figure 4.2 shows the position of the minimum, v_B, as a function of the field strength. Notice that, as expected, v_B grows with the field strength, signaling magnetic catalysis.

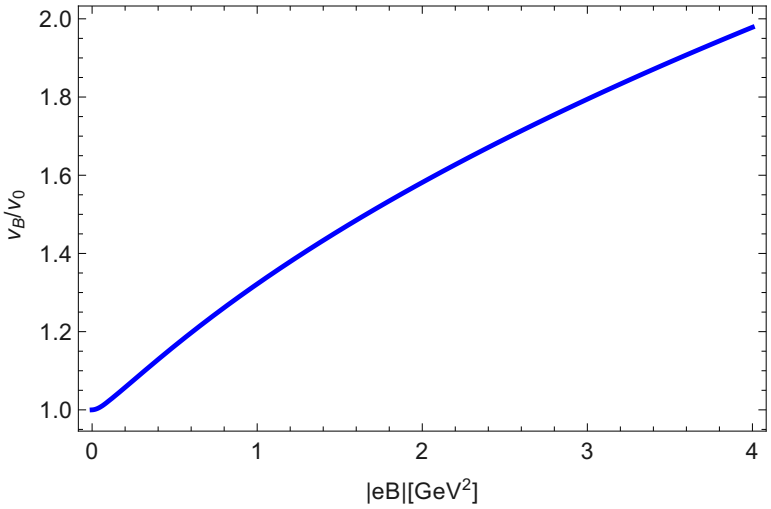

Figure 4.2: Magnetic modification to the vacuum expectation value, v_B, as a function of the field strength. For the calculation we use $m_0 = 140$ MeV, $\lambda = 3.67$, $g = 0.46$, and correspondingly $m_\sigma = 435$ MeV, $a = 256$ MeV and $v_0 = 152$ MeV. The choice of these parameters will be explained further on.

With the magnetic corrections to the vacuum expectation value at hand, we now turn our attention to computing the rest of the elements, starting from the magnetic modifications to the self-energy.

4.2 Neutral pion's self-energy

The neutral pion self-energy at one loop can be determined according to the following equation

$$\Pi(B,q) = \sum_f \Pi_{f\bar{f}}(B,q) + \Pi_{\pi_-}(B) + \Pi_{\pi_+}(B) + \Pi_{\pi_0} + \Pi_\sigma. \tag{4.19}$$

The five terms on the right-hand side of Eq. (4.19) correspond to the Feynman diagrams contributing to this self-energy at one-loop order. The subindices represent the kind of particles in the loop. The contributions to this self-energy are: the quark-antiquark loop, $\Pi_{f\bar{f}}$,

depicted in Fig. 4.3 and the boson loops, $\Pi_{\pi_\pm}$, Π_{π_0}, Π_σ. The Feynman diagram corresponding to Π_{π^-} is depicted in Fig. 4.4, and we single it out from the neutral boson loops, since this diagram, together with the diagram corresponding to its charge conjugate (CC) Π_{π_+}, are the only ones modified by the presence of the magnetic field. Diagrams with neutral bosons in the loop contribute only to vacuum renormalization and not to the magnetic properties of the system. Therefore, hereafter we do not consider the latter for the description of the magnetic modifications of the pion self-energy.

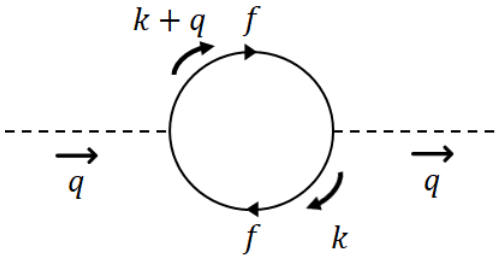

Figure 4.3: Feynman diagram showing the one-loop contributions from fermions to the neutral pion self-energy in the LSMq.

First, we concentrate on the contribution from the quark-antiquark loop for a single quark species, given explicitly by

$$-i\Pi_{f\bar{f}}(B,q) = -g^2 \int \frac{d^4k}{(2\pi)^4} \mathrm{Tr}[\gamma_5 iS_f(k)\gamma_5 iS_f(k+q)] + \mathrm{CC}, \tag{4.20}$$

Since both particles flow with the same charge around the loop, the Schwinger phase vanishes. The quark propagator in the presence of a magnetic field, iS_f, is written in the strong field limit using the LLL contribution according to Eq. (3.17). The procedure to compute this contribution is shown in Appendix C and is given by

$$-i\Pi_{f\bar{f}} = \frac{ig^2|q_fB|}{2\pi^2} e^{-\frac{1}{2|q_fB|}q_\perp^2} \int_0^1 dx \left[\frac{1}{\varepsilon} + \ln(4\pi) - \gamma_E - \ln\left(\frac{\Delta_1}{\mu^2}\right) - 1 + \frac{x(1-x)q_\parallel^2 + m_f^2}{\Delta_1}\right], \tag{4.21}$$

where $\Delta_1 = x(x-1)q_\parallel^2 + m_f^2$ and μ is the ultraviolet renormalization scale. In order to capture the overall magnetic field effects for on-shell and nonmoving pions, we resort to computing the fermion contribution to the pion self-energy in the *static limit*, namely, $q_0 = m_B$ and $\vec{q} = \vec{0}$. As also discussed in Appendix C, working with the $\overline{\mathrm{MS}}$ renormalization scheme, this is explicitly given by

$$\Pi_{f\bar{f}} = \frac{g^2|q_fB|}{2\pi^2}\left[\ln\left(\frac{m_f^2}{\mu^2}\right) - \frac{2m_B}{\sqrt{4m_f^2 - m_B^2}}\mathrm{arccsc}\left(\frac{2m_f}{m_B}\right)\right]. \tag{4.22}$$

Notice that Eq. (4.22) has an explicit dependence on μ as usual in one-loop calculations where, in order to regulate the integration, such a scale needs to be introduced. In the strong field limit, μ needs to be chosen in such a way that this becomes the largest of all energy scales, larger than the gap $\sqrt{2|eB|}$, between the LLL and the first excited Landau level. To accomplish this constraint, we chose $\mu^2 = 2|eB| + m_0^2$. A more in-depth discussion

about this choice is provided in the next section. With this choice, the contribution from the quark-antiquark loop for a single quark species becomes

$$\Pi_{f\bar{f}} = \frac{g^2|q_f B|}{2\pi^2}\left[\ln\left(\frac{m_f^2}{2|eB|+m_0^2}\right) - \frac{2m_B}{\sqrt{4m_f^2-m_B^2}}\operatorname{arccsc}\left(\frac{2m_f}{m_B}\right)\right]. \tag{4.23}$$

We proceed to compute the charged boson loop contribution to the pion self-energy. This

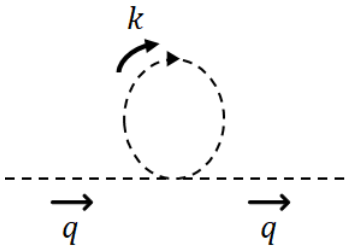

Figure 4.4: Feynman diagram showing the one-loop contribution from charged pions to the neutral pion self-energy in the LSMq.

can be written as

$$-i\Pi_{\pi^\pm} = \int \frac{d^4k}{(2\pi)^4}(-2i\lambda)iD_{\pi^\pm}(k). \tag{4.24}$$

Notice that since the initial and final loop space-time points in the tadpole Feynman diagram coincide, the Schwinger phase vanishes. To compute Eq. (4.24) in the strong field limit, we use the charged boson propagator in LLL approximation as Eq. (3.18). The procedure to compute this contribution is shown in Appendix C. Choosing $\mu^2 = 2|eB|+m_0^2$ [11], the result can be expressed as

$$\Pi_{\pi^\pm} = -\frac{\lambda|eB|}{4\pi^2}\ln\left(\frac{|eB|+m_0^2}{2|eB|+m_0^2}\right). \tag{4.25}$$

Once we determine the magnetic corrections to the vacuum expectation value of the sigma field and the self-energy we conclude the one-loop calculations studying the magnetic modifications to the couplings.

4.3 Magnetic corrections to the boson self-coupling

The corrections induced by an external magnetic field to the boson self-coupling, λ, can be obtained at one-loop order from the Feynman diagram depicted in Fig. 4.5, where the loop pions are the charged ones. In our approach, the external particles do not experience the effects of the magnetic field so that they can be adressed properly as plane waves. The only particles affected by the magnetic background are the charged, loop particles. With this idea we intend to capture the distinction between the modification of the interaction, that in a perturbative approach is a short distance effect, from the asymptotic propagation of the external particles, which corresponds to a long distance effect. Therefore, since the correction we look for is, in this sense, independent of whether the external bosons are charged

or neutral, the electric charge of the external particles is irrelevant. Thus, the correction we look for is written as

$$-i6\lambda\Gamma^B_\lambda = \int \frac{d^4k}{(2\pi)^4}(-2i\lambda)iD_{\pi^-}(k)(-2i\lambda)iD_{\pi^-}(k+p+r) + \text{CC}, \tag{4.26}$$

where CC denotes the charge conjugate term and the subscript in the boson propagator indicates the propagating species. Since the loop in Fig. 4.5 involves the same propagating particle, the Schwinger phase vanishes. According to the explicit computation shown in

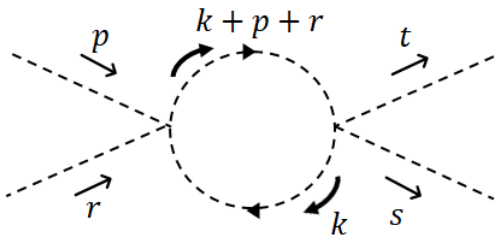

Figure 4.5: Feynman diagram representing the magnetic correction to the boson self-coupling at one loop. The loop particles are considered as electrically charged whereas the external ones can be either charged or neutral.

Appendix D and in the *static* limit $p_0, r_0 \to 0$, $\vec{p} = \vec{r} = \vec{0}$, we have

$$\Gamma^B_\lambda = -\frac{\lambda}{12\pi^2}\left[\frac{1}{\varepsilon} - \gamma_E + \ln(4\pi) - \psi^0\left(\frac{|q_bB| + m_0^2}{2|q_bB|}\right) + \ln\left(\frac{\mu^2}{2|q_bB|}\right)\right], \tag{4.27}$$

where ψ^0 is the digamma function and $|q_bB| = |eB|$ for the charged pions. According to the modified minimal subtraction scheme $\overline{\text{MS}}$, the first three terms in Eq. (4.27) are associated to the corresponding vertex counter-term. Consequently, the finite magnetic correction to the boson self-coupling is given by

$$\Gamma^B_\lambda = -\frac{\lambda}{12\pi^2}\left[\ln\left(\frac{\mu^2}{2|eB|}\right) - \psi^0\left(\frac{|eB| + m_0^2}{2|eB|}\right)\right]. \tag{4.28}$$

As can be seen in Eq. (4.28), the arbitrary field strength result depends on the ultraviolet renormalization scale μ. With the aim of clarifying an appropriate choice of this scale, we study the correction to the couplings in the limits when $|eB| \to \infty$ and $|eB| \to 0$. First, in the strong field limit where, as a good approximation, one can consider just the lowest Landau level contribution from Eq. (3.18) with Eq. (4.26), and working also in the static limit (with $p_0, r_0 \to 0$), the magnetic correction to the boson self-coupling in the LLL is given by

$$\Gamma^{LLL}_\lambda = -\frac{\lambda}{6\pi^2}\frac{|eB|}{|eB| + m_0^2}, \tag{4.29}$$

which is independent of μ. In the second place, in the absence of a magnetic field, the one-loop correction to the boson self-coupling can be determined from Eq. (4.28) taking the limit $|eB| \to 0$ and is given by

$$\Gamma_\lambda = -\frac{\lambda}{12\pi^2}\ln\left(\frac{\mu^2}{m_0^2}\right). \tag{4.30}$$

A comparison of both limits with the arbitrary result was studied in Ref. [11], and it was concluded that it is necessary that μ depends on $|eB|$ in order to be consistent with Eq. (4.30) and Eq. (4.29). In fact, the match is obtained when μ^2 is explicitly chosen as $\mu^2 = m_0^2 + 2|eB|$, for which the arbitrary field strength result becomes

$$\Gamma_\lambda^B = -\frac{\lambda}{12\pi^2}\left[\ln\left(\frac{m_0^2+2|eB|}{2|eB|}\right) - \psi^0\left(\frac{|eB|+m_0^2}{2|eB|}\right)\right]. \tag{4.31}$$

With this choice, the result reproduces the behavior of the coupling in both extreme limiting

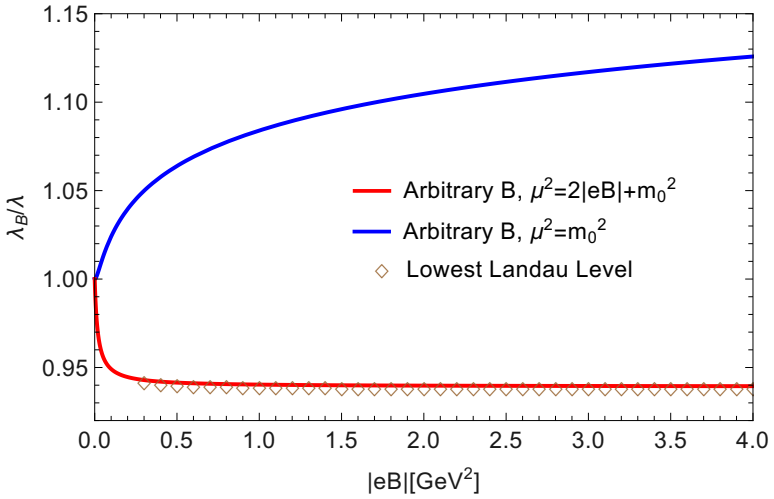

Figure 4.6: Ratio between the magnetic field dependence of the effective boson self-coupling $\lambda_B = \lambda(1+\Gamma_\lambda^B)$ and the vacuum self-coupling in the arbitrary field approach and the strong field limit, both computed in the static limit (with $p_0, r_0 \to 0$). For the calculation we use $\lambda = 3.67$ and $m_0 = 0.140$ GeV. Shown are the cases where for the arbitrary field intensity calculation, the ultraviolet renormalization scale μ^2 is taken as $m_0^2 + 2|eB|$ (red line) and a fixed value $\mu^2 = m_0^2$ (blue line). For both cases the self-coupling relative change from the vacuum value is rather small.

values of $|eB|$ and it is also compatible with the behavior of the coupling found in Ref. [7] for the weak field case. This behavior is shown in Fig. 4.6 where we plot the ratio between the effective, magnetic-field-dependent boson self-coupling $\lambda_B = \lambda\left(1+\Gamma_\lambda^B\right)$ as a function of the field strength and the vacuum boson self-coupling. In contrast, when μ is taken at a fixed value, the arbitrary field result does not match the LLL case. We interpret this result as signaling that when the field strength is the largest energy scale, μ needs to be taken also as this large scale since otherwise the computation is not consistent when the strength of the magnetic field surpasses a given fixed scale. At the same time, when the field strength vanishes, the only remaining energy scale is the pion mass and μ needs to be taken solely as this energy scale. Equally important, $2|eB|$ corresponds to the square of the energy gap between Landau levels, and, thus, that in order for μ to correspond to the largest energy scale, it is important that for large values of the field strength, μ^2 is taken as the square of this energy gap. In contrast, as also shown in Fig. 4.6, the usual prescription, whereby one just subtracts the vacuum correction, represented by the blue line computed with $\mu^2 = m_0^2$, behaves opposite to what is expected from the result obtained using the LLL propagator.

4.4 Magnetic corrections to the boson-fermion coupling

The magnetic corrections to the boson-fermion coupling g at one-loop level can be obtained from the sum of the three Feynman diagrams depicted in Fig. 4.7. Since the correction

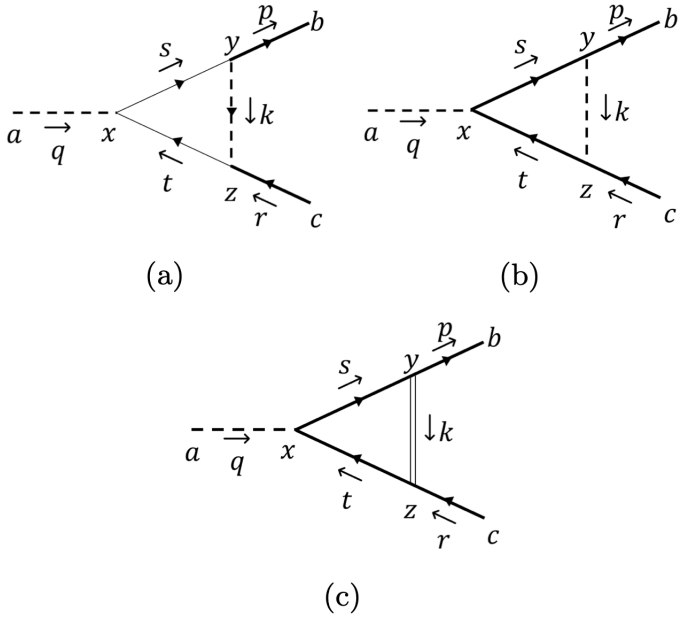

Figure 4.7: Feynman diagrams that contribute to the boson-fermion coupling at one-loop order. The diagrams show the case with a neutral pion and two u quarks as the external particles. Here x, y and z are internal points, while a, b and z are external points in configuration space.

can be obtained from the sum of the allowed diagrams coupling one boson and two quarks, here we consider the magnetic correction to the boson-fermion coupling for the choice of external particles shown in Fig. 4.7. Also, as discussed in the previous section, the use of propagators in the LLL approximation provides a reliable description in the strong field limit, we hereby restrict ourselves to this case using the LLL approximation, Eq. (3.18), for the boson propagator and Eq. (3.17) for the fermion propagator.

We start by computing the contribution from the diagram in Fig. 4.7(a). This diagram is associated with the quantity $I^B_{1,g}$ which is explicitly given by

$$\begin{aligned} I^B_{1,g} &= \int d^4x\, d^4y\, d^4x \int \frac{d^4s}{(2\pi)^4}\frac{d^4t}{(2\pi)^4}\frac{d^4k}{(2\pi)^4}\, e^{i\Phi_{1,l}} e^{-ip\cdot y}\left(\sqrt{2}g\gamma^5\right) e^{-is\cdot(x-y)} iS_d(s) \\ &\times \left(-g\gamma^5\right) e^{iq\cdot x} e^{-it\cdot(z-x)} iS_d(t)\left(\sqrt{2}g\gamma^5\right) e^{-ik\cdot(y-z)} iD_{\pi^-}(k) e^{ir\cdot z} + \text{CC}. \end{aligned} \tag{4.32}$$

The information from the Schwinger phases is contained in the function $\Phi_{1,l}(x,y,z)$. This function depends on the space-time points located at the vertices. For the calculation to have a solid physical meaning, this phase should be a gauge-invariant quantity. We proceed to show this fact explicitly. Notice that the *total* Schwinger phase $\Phi_{1,t}$ associated to the Feynman diagram in Fig. 4.7(a), contains not only the information of the space-time points at the interaction vertices x, y, z, but also the one coming from the *external* space-time points

a, b, c. Therefore $\Phi_{1,t}$ is given explicitly by

$$\Phi_{1,t} = \Phi_d(x,y) + \Phi_{\pi^-}(y,z) + \Phi_d(z,x) + \Phi_u(y,b) + \Phi_u(c,z). \tag{4.33}$$

Using Eq. (3.7) with Eq. (4.33), we have

$$\Phi_{1,t} = -\frac{1}{2}q_d F_{\mu\nu}\left(y^\mu x^\nu + x^\mu z^\nu\right) - \frac{1}{2}q_{\pi^-}F_{\mu\nu}z^\mu y^\nu - \frac{1}{2}q_u F_{\mu\nu}\left(b^\mu y^\nu + z^\mu c^\nu\right) + q_u[\Lambda(b) - \Lambda(c)]. \tag{4.34}$$

It is worth pointing out that terms depending on Λ evaluated at the internal space-time points add up to zero. Therefore, the integration over the configuration space becomes independent of the gauge choice. However, this would not be the case when we just consider the phase factors associated to the particles within the loop, since the result of the integration would then become gauge dependent. This observation is essential since otherwise one faces a non-conservation of electric charge at each vertex when just considering the phases within the loop. On the other hand, Eq. (4.34) contains a mixing between the phases associated to loop particles, $\Phi_{1,l}$, and the phases from external particles, Φ_{ext}, where the last term is associated to the external charged lines in the diagram and can be written as

$$\Phi_{ext} = -\frac{1}{2}q_u F_{\mu\nu}\left(b^\mu x^\nu + x^\mu c^\nu\right) + q_u[\Lambda(b) - \Lambda(c)]. \tag{4.35}$$

In order to separate these contributions as

$$\Phi_{1,t} = \Phi_{1,l} + \Phi_{ext}, \tag{4.36}$$

we resort to considering that the external particles can be described as plane waves. Physically, this means that we consider the propagation of the external particles during short distances and times. In this manner we neglect long distance effects introduced when the magnetic field acts on the external particles. Therefore, we can take $y^\mu \approx b^\mu$ and $z^\mu \approx c^\mu$ such that

$$\Phi_{1,t} = -\frac{1}{2}q_u F_{\mu\nu}\left(b^\mu x^\nu + x^\mu c^\nu\right) + q_u[\Lambda(b) - \Lambda(c)] - \frac{1}{2}q_{\pi^-}F_{\mu\nu}\left(y^\mu x^\nu + z^\mu y^\nu + x^\mu z^\nu\right). \tag{4.37}$$

Using this approximation we can separate the phase factors coming from external and internal, loop particles. Thus, for the computation of the magnetic field correction for the coupling g, we need only to account for the last term in Eq. (4.37), whereas the first term and second term in Eq. (4.37) are associated to the external phase given by Eq. (4.35). Therefore, we have

$$\Phi_{1,l} = -\frac{1}{2}q_{\pi^-}F_{\mu\nu}\left(y^\mu x^\nu + z^\mu y^\nu + x^\mu z^\nu\right). \tag{4.38}$$

It is important to note that the contribution from the Schwinger phase is gauge-invariant. Using that $F_{21} = -F_{12} = |B|$ and $q_{\pi^-} = -|e|$, we get

$$\Phi_{1,l} = \frac{1}{2}|eB|\varepsilon_{ij}\left(x_i y_j + y_i z_j + z_i x_j\right), \quad i,j = 1,2, \tag{4.39}$$

where ε_{ij} is the Levi-Civita symbol. Having identified the Schwinger phase contribution, we can perform the integration over coordinates. Upon doing so, we obtain the energy-momentum conservation for the external particles, and can write

$$I^B_{1,g} = (2\pi)^4\delta^{(4)}(p - r - q)g\gamma^5\Gamma^B_{1,g}, \tag{4.40}$$

where $g\gamma^5\Gamma_{1,g}$ is identified as the contribution to the magnetic field correction to the vertex, given explicitly by

$$\begin{aligned} g\gamma^5\Gamma^B_{1,g} &= \frac{1}{\pi^2|eB|^2}\int d^2s_\perp d^2t_\perp \frac{d^4k}{(2\pi)^4}\left(\sqrt{2}g\gamma^5\right) iS_d(k_\parallel+p_\parallel,s_\perp)\left(-g\gamma^5\right) iS_d(k_\parallel+r_\parallel,t_\perp) \\ &\times \left(\sqrt{2}g\gamma^5\right) iD_{\pi^-}(k_\parallel,k_\perp)e^{i\frac{2}{|eB|}\varepsilon_{ij}(s-q-t)_i(s-p-k)_j} + \text{CC}. \end{aligned} \tag{4.41}$$

Following the procedure explicitly shown in Appendix E and the static limit $p_0 = r_0 = m_f$ and $\vec{p} = \vec{r} = \vec{0}$, we get

$$\Gamma^{LLL}_{1,g} = \frac{g^2|eB|}{16\pi^2 m_f^2}\int_0^1 du \frac{u}{u^2+\alpha(1-u)}\left[1+\frac{(2-u)u}{u^2+\alpha(1-u)}\right], \tag{4.42}$$

where $\alpha = (m_0^2+|eB|)/m_f^2$.

We proceed with the contribution from the Feynman diagram depicted in Fig. 4.7(b). This contribution can be obtained from the function $I^B_{2,g}$, which can be written as follows

$$\begin{aligned} I^B_{2,g} &= \int d^4x\, d^4y\, d^4z \int \frac{d^4s}{(2\pi)^4}\frac{d^4t}{(2\pi)^4}\frac{d^4k}{(2\pi)^4} e^{i\Phi_{2,l}} e^{-ip\cdot y}\left(g\gamma^5\right) e^{-is\cdot(x-y)} iS_u(s) \\ &\times \left(g\gamma^5\right) e^{iq\cdot x} e^{-it\cdot(z-x)} iS_u(t)\left(g\gamma^5\right) e^{-ik\cdot(y-z)} iD_{\pi^0}(k) e^{ir\cdot z} + \text{CC}. \end{aligned} \tag{4.43}$$

In a similar fashion, we first compute the Schwinger phase associated to the whole diagram in Fig. 4.7(b), namely,

$$\Phi_{2,t} = \Phi_u(x,y) + \Phi_u(z,x) + \Phi_u(y,b) + \Phi_u(c,z). \tag{4.44}$$

Using Eq. (3.7) with Eq. (4.44), we have

$$\Phi_{2,t} = -\frac{1}{2}F_{\mu\nu}q_u\left(y^\mu x^\nu + b^\mu y^\nu + x^\mu z^\nu + z^\mu c^\nu\right) + q_u\left[\Lambda(b)-\Lambda(c)\right]. \tag{4.45}$$

Once again terms that depend on Λ, evaluated at internal points, cancel out. On the other hand, the Schwinger phase associated to the tree-level diagram is given by Eq. (4.35). Adding and subtracting the first term from this equation to Eq. (4.45), we have

$$\begin{aligned} \Phi_{2,t} &= -\frac{1}{2}F_{\mu\nu}q_u\left(y^\mu x^\nu + b^\mu y^\nu + x^\mu z^\nu + z^\mu c^\nu\right) + q_u\left[\Lambda(b)-\Lambda(c)\right] \\ &- \frac{1}{2}q_u F_{\mu\nu}\left(b^\mu x^\nu + x^\mu c^\nu\right) + \frac{1}{2}q_u F_{\mu\nu}\left(b^\mu x^\nu + x^\mu c^\nu\right). \end{aligned} \tag{4.46}$$

Assuming that $y^\mu \approx b^\mu$ and $z^\mu \approx c^\mu$ (short space-time interval propagation after the interaction), we get

$$\Phi_{2,t} = -\frac{1}{2}q_u F_{\mu\nu}\left(b^\mu x^\nu + x^\mu c^\nu\right) + q_u\left[\Lambda(b)-\Lambda(c)\right]. \tag{4.47}$$

This result coincides with Eq. (4.35). Therefore, we can conclude that the Schwinger phase associated to the loop particles vanishes

$$\Phi_{2,l} = 0. \tag{4.48}$$

Upon integration over configuration space, we are able to identify the contribution to the magnetic correction from this diagram, $g\gamma^5\Gamma_{2,g}$, as

$$I^B_{2,g} = (2\pi)^4\delta^{(4)}(p-r-q)g\gamma^5\Gamma_{2,g}. \tag{4.49}$$

Again, notice that using this approximation we recover the energy-momentum conservation for the external particles, whereas the magnetic correction is associated to the loop and can be expressed as

$$g\gamma^5\Gamma^B_{2,g} = \int \frac{d^4k}{(2\pi)^4}\left(g\gamma^5\right) iS_u(k+p)\left(g\gamma^5\right) iS_u(k+r)\left(g\gamma^5\right) iD_{\pi^0}(k) + \text{CC}. \tag{4.50}$$

The computation of this quantity is explicitly performed in Appendix E in the strong field limit and can be expressed as

$$\Gamma^{LLL}_{2,g} = -\frac{g^2}{2\pi^2 m_f^2}\int_0^1 du\int_0^\infty dk_\perp\; k_\perp e^{-\frac{3k_\perp^2}{|eB|}}\frac{u}{u^2+\beta(1-u)}\left[1+\frac{(2-u)u}{u^2+\beta(1-u)}\right], \tag{4.51}$$

where $\beta = (k_\perp^2+m_0^2)/m_f^2$.

The diagram in Fig. 4.7(c) can be obtained from the function $I^B_{3,g}$, given explicitly by

$$\begin{aligned} I^B_{3,g} &= \int d^4x\, d^4y\, d^4z \int \frac{d^4s}{(2\pi)^4}\frac{d^4t}{(2\pi)^4}\frac{d^4k}{(2\pi)^4} e^{i\Phi_{3,l}} e^{-ip\cdot y}\,(-ig)\, e^{-is\cdot(x-y)} iS_u(s) \\ &\times \left(g\gamma^5\right) e^{iq\cdot x} e^{-it\cdot(z-x)} iS_u(t)\,(-ig)\, e^{-ik\cdot(y-z)} iD_\sigma(k) e^{ir\cdot z} + \text{CC}. \end{aligned} \tag{4.52}$$

In a similar fashion, one can compute the Schwinger phase from this loop, $\Phi_{3,l}(x,y,z)$. It is easy to see that this phase satisfies $\Phi_{3,t} = \Phi_{2,t}$ and therefore, the internal Schwinger phase vanishes when considering short-range propagation of the external particles, namely,

$$\Phi_{3,l} = 0. \tag{4.53}$$

After performing the integration over the configuration space, we obtain a the relation between $I^B_{3,g}$ and the contribution to the magnetic correction to the boson-fermion coupling, $g\gamma^5\Gamma_{3,g}$, given by

$$I^B_{3,g} = (2\pi)^4\delta^{(4)}(p-r-q)g\gamma^5\Gamma_{3,g}, \tag{4.54}$$

with

$$g\gamma^5\Gamma^B_{3,g} = \int \frac{d^4k}{(2\pi)^4}\,(-ig)\, iS_u(k+p)\left(g\gamma^5\right) iS_u(k+r)\,(-ig)\, iD_\sigma(k) + \text{CC}. \tag{4.55}$$

Once again, using the LLL propagators and following the explicit procedure shown in Appendix E, we get

$$\Gamma^{LLL}_{3,g} = \frac{g^2}{2\pi^2 m_f^2}\int_0^1 du\int_0^\infty dk_\perp\; k_\perp e^{-\frac{3k_\perp^2}{|eB|}}\frac{u}{u^2+\gamma(1-u)}\left[1+\frac{(2-u)u}{u^2+\gamma(1-u)}\right], \tag{4.56}$$

where $\gamma = (k_\perp^2+m_\sigma^2)/m_f^2$.

The total magnetic correction to the boson-fermion coupling in the strong field limit is given by the sum of the three contributions, namely,

$$\Gamma_g^{LLL} = \Gamma_{1,g}^{LLL} + \Gamma_{2,g}^{LLL} + \Gamma_{3,g}^{LLL}. \tag{4.57}$$

The effective boson-fermion coupling, g^{eff} is thus given by

$$g_B = g\left(1 + \Gamma_g^{LLL}\right). \tag{4.58}$$

Figure 4.8 shows the behavior of the boson-fermion coupling as a function of the field strength. For the calculation we set $m_0 = 0.140$ GeV, $m_f = 0.3$ GeV and $m_\sigma = 0.4$, 0.6 GeV. Notice that the coupling decreases monotonically over a large range of the field strength. However, the relative change is rather small.

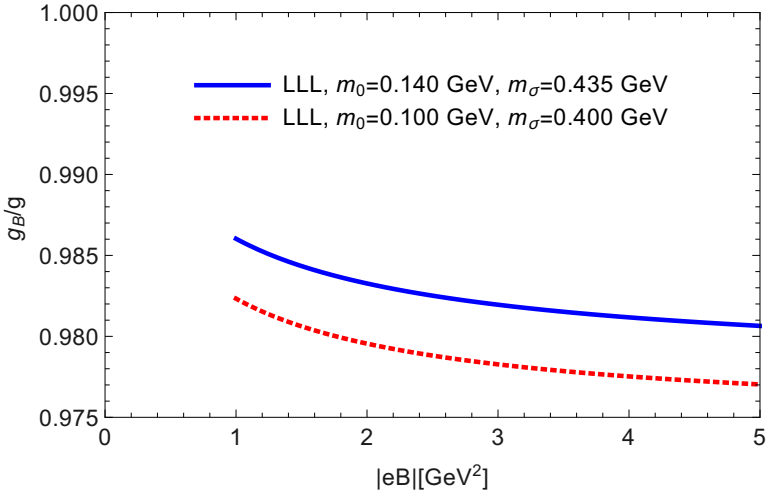

Figure 4.8: Magnetic field dependence of the effective boson-fermion coupling $g_B = g(1+\Gamma_g^B)$ in the static limit and the strong field approximation. For the calculation we used $g = 0.46$, $m_f = 0.07$ GeV and the two values $m_\sigma = 0.400$ GeV and 0.435 GeV and $m_0 = 0.100$ GeV and 0.140 GeV. In both cases g_B monotonically decreases in an interval $|eB| = 1 - 5$ GeV^2.

In this chapter we determined the behavior of the vacuum expection value for an arbitrary field strength and the neutral pion self-energy, the boson self-coupling and the boson-fermion coupling in the strong field limit. These elements allow us to study the magnetic corrections to the neutral pion mass through its dispersion relation. This analysis is performed in the next chapter.

Chapter 5

Magnetic modifications to the neutral pion mass

In this chapter we study the dispersion relation of the neutral pion in Eq. (4.1) at one-loop order in order to determine the magnetic-field-dependent neutral pion mass. Furthermore, a comparison with the recent LQCD results is performed. We employ a proper set of parameters in agreement with their choice for the physical pion mass in vacuum. The results presented below were reported in Ref. [12].

Hereafter, we consider Eq. (4.1) in the limit where $\vec{q} \to \vec{0}$ and $q_0 \to m_B$, namely,

$$m_B^2 = m_0^2(\lambda_B, v_B) + \Pi(B, q_0 = m_B, \vec{q} = 0; \lambda_B, g_B, v_B), \tag{5.1}$$

where, in order to incorporate the magnetic-field-dependent boson self-coupling and vacuum expectation value in the three-level pion mass, we write

$$m_0^2(\lambda_B, v_B) = \lambda_B v_B^2 - a^2. \tag{5.2}$$

The expressions in Eq. (2.9) reduce the parameter space in the LSMq so that there are four free parameters associated with physical quantities in vacuum, namely, m_0, m_f, λ and g. Additionally, we consider that in the absence of baryons, the constituent quark mass is such that $m_0 = 2m_f$. With this choice, the only free parameters are λ and g. We have explored a large range for these parameters and hereby we show the results for the set that best describes simultaneously the LQCD data of Refs. [48, 49]. Since these works report their findings for different values of the vacuum pion mass, we also vary this mass, and, consequently, the rest of the dependent parameters have to be changed to suit these choices. In particular, a larger vacuum pion mass implies a larger σ mass. Thus, in the strong field limit, our results are restricted to the domain where $|eB| > m_\sigma^2$. Figure 5.1 shows the magnetic-field-dependent neutral pion mass as a function of the field strength computed for two cases: with (black dots) and without (blue diamonds) magnetic-field-dependent couplings, using as inputs $m_0 = 140$ MeV, $\lambda = 3.67$, $g = 0.46$, and, correspondingly, $m_\sigma = 435$ MeV, $a = 256$ MeV and $v_0 = 152$ MeV. The former shows a monotonic decrease, whereas the latter starts off decreasing to later on increase as a function of the field strength. This result signals the importance of including magnetic field corrections to the couplings in the calculation of the magnetic-field-dependent neutral pion mass.

In order to compare with LQCD simulations, which are implemented for different values of the vacuum pion mass, Fig. 5.2 shows the magnetic-field-dependent neutral pion mass as

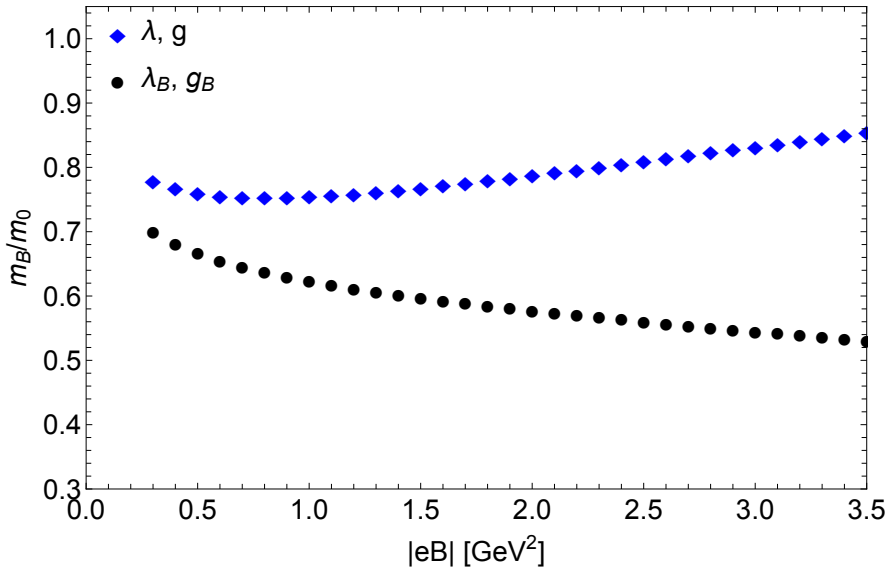

Figure 5.1: Magnetic modification to the neutral pion mass, for two different cases: Blue diamonds correspond to tree-level couplings, and black dots correspond to magnetic-field-dependent couplings. The calculation using tree-level couplings starts off decreasing to later on increase, whereas the calculation using magnetic-field-dependent couplings decreases monotonically as a function of the field strength. For the calculation we use $m_0 = 140$ MeV, $\lambda = 3.67$, $g = 0.46$, and, correspondingly, $m_\sigma = 435$ MeV, $a = 256$ MeV, and $v_0 = 152$ MeV.

a function of the field strength when varying the input vacuum pion mass. Shown are three cases: $m_0 = 140$ MeV (black dots), $m_0 = 220$ MeV (blue triangles) and $m_0 = 415$ MeV (red diamonds). Notice that, as the physical pion mass decreases, the corresponding magnetic-field-dependent pion mass also decreases and that all cases show a monotonic decrease as a function of the field strength, in agreement with the LQCD findings.

To make direct contact with LQCD data, Fig. 5.3 shows the results for the magnetic-field-dependent neutral pion mass as a function of the field strength using as input $m_0 = 415$ MeV and with $\lambda = 3.67$ and $g = 0.46$, compared to the results from Ref. [48]. The data points correspond to the π_d (blue diamonds) and π_u (red diamonds) masses computed also using as input $m_0 = 415$ MeV. Our calculation does a nice description of the data average, particularly for the largest field strengths. Figure 5.4 shows also a comparison of our calculation with the LQCD calculation of Ref. [49], this time computed with $m_0 = 220$ MeV as input together with $\lambda = 3.67$ and $g = 0.46$. The data points correspond to the π_d (blue diamonds) and π_u (red diamonds) masses computed also using as input $m_0 = 220$ MeV. Once again, we notice that our calculation does a nice job describing the average of the LQCD masses, particularly for large values of the field strength.

Finally, Fig. 5.5 shows a comparison of our calculation with the results of the LQCD calculations from Refs. [48, 49]. The data points correspond to the lowest reached values of each LQCD calculation, $m_0 = 415$ MeV for the former and $m_0 = 220$ MeV for the latter. The calculation (black dots) is performed with $m_0 = 140$ MeV as input, together with $\lambda = 3.67$ and $g = 0.46$. The result of the calculation using as input the physical pion mass in vacuum lies below the LQCD points. In this sense, this result can be considered as our prediction when and if LQCD techniques can be performed for a physical vacuum pion mass.

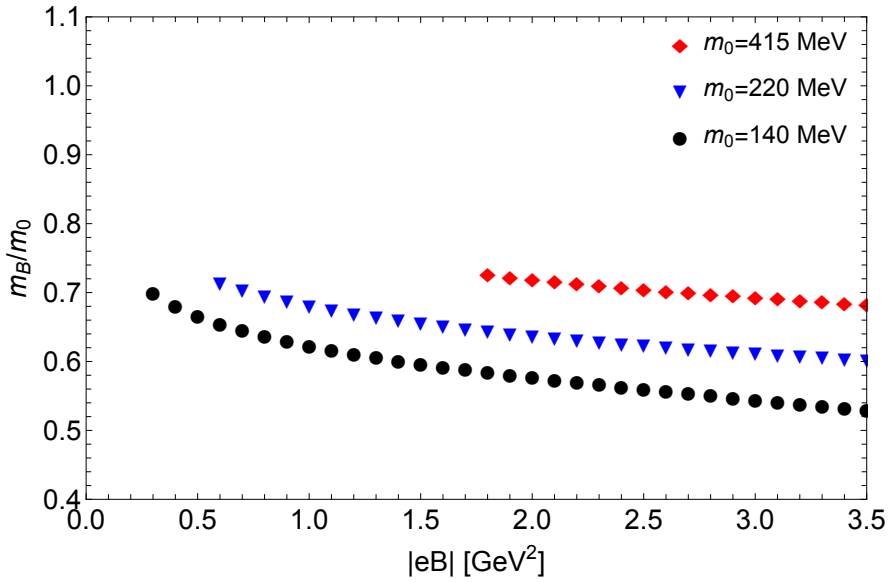

Figure 5.2: Magnetic modification to the neutral pion mass for three different values of pion mass in vacuum: black dots, $m_0 = 140$ MeV, blue triangles, $m_0 = 220$ MeV and red diamonds $m_0 = 415$ MeV. Notice that, as the physical pion mass decreases the corresponding magnetic-field-dependent pion mass also decreases and that all cases show a monotonic decrease as a function of the field strength, in agreement with the recent LQCD findings.

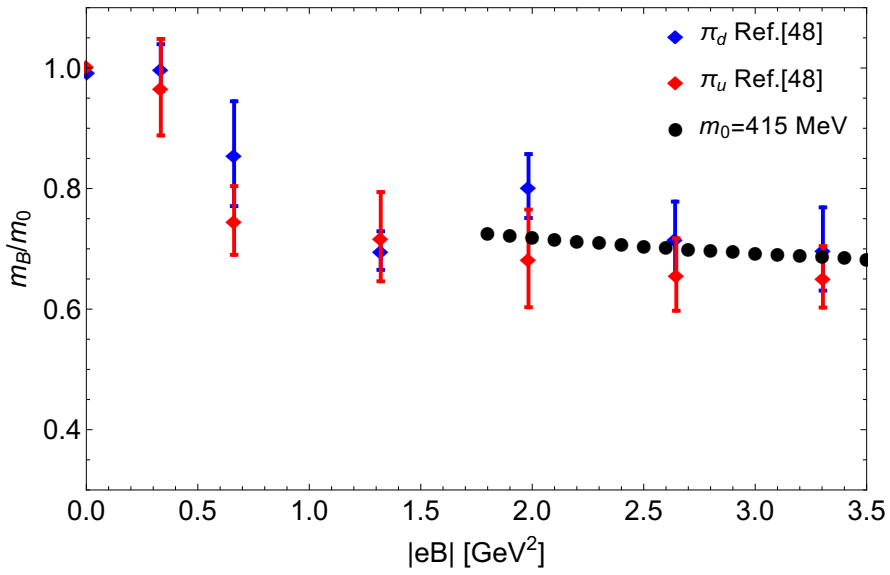

Figure 5.3: Magnetic modification to the neutral pion mass. Blue and red diamonds correspond to the masses of π_d and π_u reported by LQCD in Ref. [48] with $m_0 = 415$ MeV. Black dots are the result from Eq. (5.1) with $m_0 = 415$ MeV, $\lambda = 3.67$, $g = 0.46$, and, correspondingly, $m_\sigma = 1291$ MeV, $a = 758$ MeV and $v_0 = 451$ MeV.

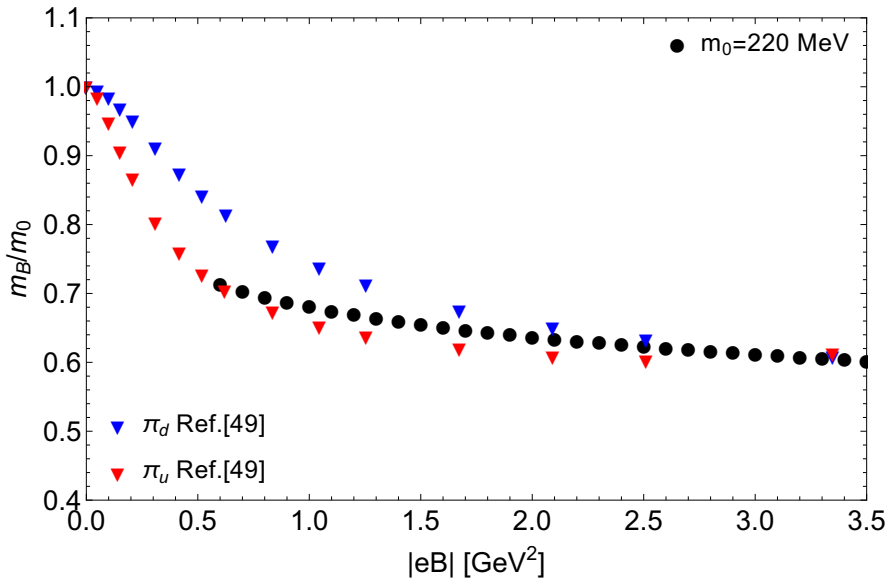

Figure 5.4: Magnetic modification to the neutral pion mass. Blue and red triangles correspond to the masses of π_d and π_u reported by LQCD in Ref. [49] with $m_0 = 220$ MeV. Black dots are the result from Eq. (5.1) with $m_0 = 220$ MeV, $\lambda = 3.67$, $g = 0.46$, and, correspondingly, $m_\sigma = 684$ MeV, $a = 402$ MeV and $v_0 = 239$ MeV.

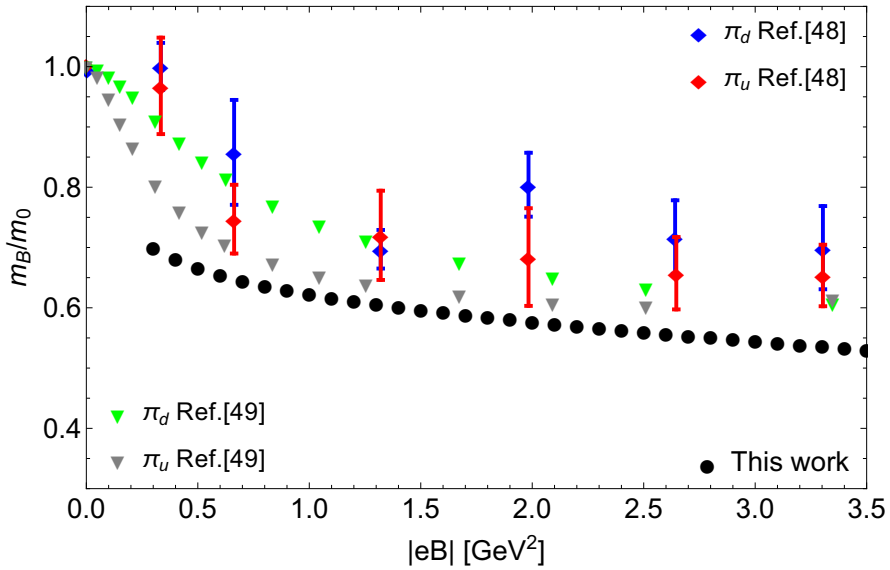

Figure 5.5: Magnetic modification to the neutral pion mass. Blue and red diamonds correspond to the masses of π_d and π_u reported by LQCD in Ref. [48] with $m_0 = 415$ MeV. Green and gray triangles correspond to the masses of π_d and π_u reported by LQCD in Ref. [49] with $m_0 = 220$ MeV. Black dots are the result of Eq. (5.1) with $m_0 = 140$ MeV, $\lambda = 3.67$, $g = 0.46$, and, correspondingly, $m_\sigma = 435$ MeV, $a = 256$ MeV and $v_0 = 152$ MeV. As expected, when for the calculation we use as input the physical pion mass $m_0 = 140$ MeV, the theoretical curve lies below the LQCD data which were obtained using larger vacuum pion masses.

Chapter 6

Conclusions

The Linear Sigma Model with quarks (LSMq) is an effective model of QCD in the low-energy regime. This model describes the interaction among light mesons and quarks and captures the chiral symmetry of QCD. Since the masses of the particles species in this model have a dynamical nature through the chiral symmetry breaking, the main objective of this work is to provide an appropriate description of the magnetic field effects in the neutral pion mass at one-loop level by using charged particle propagators in the presence of a uniform and constant magnetic field.

The approach adopted consists of the proper inclusion of the purely magnetic field modifications on the model couplings, the σ vacuum expectation value and the neutral pion self-energy combined with a suitable set of parameters. Following this path the predictions from the LSMq subject to a magnetized medium reproduce the magnetic field dependence of the neutral pion mass reported by recent LQCD calculations. Additionally, a monotonically increasing behavior as a function of the field strength was determined for the σ vacuum expectation value which is to be expected on general grounds given by the well-known magnetic catalysis phenomenon.

As has been previously discussed, the boson self-coupling and the boson-fermion coupling play a significant role for the monotonically decreasing behavior of the neutral pion mass. For the former, the results for an arbitrary field strength, as well as in the strong field are provided in detail. In this case, the full magnetic field result for the boson self-coupling allowed us to study its ultraviolet scale dependence, considering the strong field limit and the result in absence of magnetic field we found an appropriate choice for the renormalization scale that produces the expected behavior for both extreme limits and is supported by a reliable physical interpretation. For the latter, we solely consider a calculation in the strong field limit. Furthermore, we have shown that when considering that the external charged particles propagate during short space-time intervals, the effects coming from the Schwinger phase become gauge invariant and the energy-momentum conservation can be factored out from the vertex function.

By comparing to the LQCD results for the smallest pion mass allowed by that technique, we obtain that when the physical pion mass is used in our approach, the magnetic-field-dependent neutral pion mass curve lies a bit below the LQCD data. In this sense, this result is our prediction if the LQCD techniques allow for calculations using the physical vacuum pion mass.

Finally, the results in this work can be used to address whether this approach can also

reproduce the magnetic field behavior of the charged pion mass with the same set of parameters. Other possible physical scenarios where the results of this work can have a potential impact include the nuclear equation of state within dense and compact astrophysical objects, such as the cores of neutron stars, which are affected by magnetic-field-dependent baryon and meson masses and couplings, and the shear and bulk viscosity in quark-meson matter.

Appendix A

Regularization and Renormalization

The aim of this section is to briefly discuss the regularization and renormalization procedures and show explicitly some relations in the context of the dimensional regulatization method.

Regularization is a procedure which modifies an original quantum field theory in order to study short-distance physical effects (ultraviolet regime). Usually, when radiative corrections are considered (one-loop or higher corrections), the regularization procedures allow us to deal with divergent expressions by introducing the concept of regulator. For instance, in the dimensional regularization method, ε, is the regulator. The original theory is recovered in the limit in which the regulator goes away , $\varepsilon \to 0$, but the virtue of the regulator is that for a non-zero positive value, the result is finite. This method is widely used because it is the only known method which is Lorentz-invariant and gauge-invariant. An overview of this method is shown below.

In dimensional regularization we promote from 4 dimensions to d according to

$$\int \frac{d^4l}{(2\pi)^4} = \mu^{4-d} \int \frac{d^dl}{(2\pi)^d}, \tag{A.1}$$

where μ is the ultraviolet renormalization scale and have energy units. This variable plays an important role in the renormalization group approach and physically it can be chosen as the largest energy scale of the system.

On one hand, at the one-loop level, the calculation of Feynman diagrams in vacuum involve the relations in Eq.(A.2) and (A.3) which can be solved as a $d-$dimensional integration in Minkowski space [59]

$$\int \frac{d^dl}{(2\pi)^d} \frac{1}{(l^2-\Delta)^n} = \frac{(-1)^n i}{(4\pi)^{d/2}} \frac{\Gamma\left(n-\frac{d}{2}\right)}{\Gamma(n)} \left(\frac{1}{\Delta}\right)^{n-\frac{d}{2}}, \tag{A.2}$$

$$\int \frac{d^dl}{(2\pi)^d} \frac{l^2}{(l^2-\Delta)^n} = \frac{(-1)^{n-1} i}{(4\pi)^{d/2}} \frac{d}{2} \frac{\Gamma\left(n-\frac{d}{2}-1\right)}{\Gamma(n)} \left(\frac{1}{\Delta}\right)^{n-\frac{d}{2}-1}. \tag{A.3}$$

where n. In fact, from Eqs. (A.2) and (A.3) it can be seen that d is not necessarily an integer. On the other hand, once we incorporate a uniform and constant time external magnetic field, the propagators can be separated in structures which depend on the parallel and perpendicular momentum coordinates (relative to the magnetic field direction, where the zeroth component is included in the parallel structure) independently. Usually when one-loop level calculations are considered, the parallel structure may be divergent, while the

perpendicular structure is convergent. The prescription to promote from 4 dimensions to d in this case is usually performed in the following manner

$$\int \frac{d^4l}{(2\pi)^4} = \int \frac{d^2l_\parallel d^2l_\perp}{(2\pi)^4} = \mu^{4-d} \int \frac{d^{d-2}l_\parallel}{(2\pi)^{d-2}} \int \frac{d^2l_\perp}{(2\pi)^2}. \tag{A.4}$$

Thus, according to this separation, the general relations in Eqs.(A.2) and (A.3) can be written in $d-2$ dimensions as follows

$$\int \frac{d^{d-2}l_\parallel}{(2\pi)^{d-2}} \frac{1}{(l_\parallel^2 - \Delta)^n} = \frac{(-1)^n i}{(4\pi)^{(d-2)/2}} \frac{\Gamma\left(n - \frac{d-2}{2}\right)}{\Gamma(n)} \left(\frac{1}{\Delta}\right)^{n-\frac{d-2}{2}}, \tag{A.5}$$

$$\int \frac{d^{d-2}l_\parallel}{(2\pi)^{d-2}} \frac{l_\parallel^2}{(l_\parallel^2 - \Delta)^n} = \frac{(-1)^{n-1} i}{(4\pi)^{(d-2)/2}} \frac{d-2}{2} \frac{\Gamma\left(n - \frac{d-2}{2} - 1\right)}{\Gamma(n)} \left(\frac{1}{\Delta}\right)^{n-\frac{d-2}{2}-1}. \tag{A.6}$$

Following this path, consider Eq. (A.5) for $n = 1$

$$\mu^{4-d} \int \frac{d^{d-2}l_\parallel}{(2\pi)^{d-2}} \frac{1}{l_\parallel^2 - \Delta} = -\frac{i}{(4\pi)^{(d-2)/2}} \frac{\Gamma\left(1 - \frac{d-2}{2}\right)}{\Gamma(1)} \left(\frac{\mu^2}{\Delta}\right)^{1-\frac{d-2}{2}}, \tag{A.7}$$

taking $d = 4 - 2\varepsilon$, we get

$$\mu^{4-d} \int \frac{d^{d-2}l_\parallel}{(2\pi)^{d-2}} \frac{1}{l_\parallel^2 - \Delta} = -\frac{i}{4\pi} (4\pi)^\varepsilon \Gamma(\varepsilon) \left(\frac{\mu^2}{\Delta}\right)^\varepsilon. \tag{A.8}$$

Considering an expansion in $\varepsilon \to 0$ we are able to identify the divergent term as

$$(4\pi)^\varepsilon \Gamma(\varepsilon) \left(\frac{\mu^2}{\Delta}\right)^\varepsilon = \frac{1}{\varepsilon} + \ln(4\pi) - \ln\left(\frac{\Delta}{\mu^2}\right) - \gamma_E + \mathcal{O}(\varepsilon). \tag{A.9}$$

Thus, we get

$$\mu^{4-d} \int \frac{d^{d-2}l_\parallel}{(2\pi)^{d-2}} \frac{1}{l_\parallel^2 - \Delta} = -\frac{i}{4\pi} \left[\frac{1}{\varepsilon} + \ln(4\pi) - \ln\left(\frac{\Delta}{\mu^2}\right) - \gamma_E + \mathcal{O}(\varepsilon)\right]. \tag{A.10}$$

Furthermore, taking $n = 2$ in Eqs.(A.5) and (A.6) with $d = 4 - 2\varepsilon$

$$\mu^{4-(d-2)} \int \frac{d^{d-2}l_\parallel}{(2\pi)^{d-2}} \frac{1}{(l_\parallel^2 - \Delta)^2} = \frac{i}{(4\pi)^{1-\varepsilon}} \frac{\Gamma(1+\varepsilon)}{\Gamma(2)} \left(\frac{\mu^2}{\Delta}\right)^{1+\varepsilon}, \tag{A.11}$$

$$\mu^{2-(d-2)} \int \frac{d^{d-2}l_\parallel}{(2\pi)^{d-2}} \frac{l_\parallel^2}{(l_\parallel^2 - \Delta)^2} = -\frac{i}{(4\pi)^{1-\varepsilon}} (1-\varepsilon) \frac{\Gamma(\varepsilon)}{\Gamma(2)} \left(\frac{\mu^2}{\Delta}\right)^\varepsilon. \tag{A.12}$$

We proceed using the properties: $\Gamma(z+1) = z\Gamma(z)$, $\Gamma(2) = 1$, and an expansion in $\varepsilon \to 0$ such as the results are given by

$$\mu^{4-(d-2)} \int \frac{d^{d-2}l_\parallel}{(2\pi)^{d-2}} \frac{1}{(l_\parallel^2 - \Delta)^2} = \frac{i}{4\pi} \frac{\mu^2}{\Delta} \left[1 + \mathcal{O}(\varepsilon)\right], \tag{A.13}$$

$$\mu^{2-(d-2)} \int \frac{d^{d-2}l_\parallel}{(2\pi)^{d-2}} \frac{l_\parallel^2}{(l_\parallel^2 - \Delta)^2} = -\frac{i}{4\pi} \left[\frac{1}{\varepsilon} - \ln\left(\frac{\Delta}{4\pi\mu^2}\right) - \gamma_E - 1 + \mathcal{O}(\varepsilon)\right], \tag{A.14}$$

Finally, following a similar procedure as before, setting $n = 3$ in Eqs.(A.5) and (A.6), we have

$$\mu^{4-d}\int \frac{d^{d-2}l_{\parallel}}{(2\pi)^{d-2}}\frac{1}{(l_{\parallel}^2-\Delta)^3} = -\frac{i}{4\pi}\frac{1}{2}\frac{1}{\Delta^2}+\mathcal{O}(\varepsilon), \tag{A.15}$$

$$\mu^{4-d}\int \frac{d^{d-2}l_{\parallel}}{(2\pi)^{d-2}}\frac{l_{\parallel}^2}{(l_{\parallel}^2-\Delta)^3} = \frac{i}{4\pi}\frac{1}{2}\frac{1}{\Delta}+\mathcal{O}(\varepsilon). \tag{A.16}$$

With these expressions at hand, we are able to solve the integration which arise from the elements needed to compute the neutral pion mass at one-loop order in the strong field limit.

Naturally, it is essential to express our predictions for the physical quantities in terms of physical parameters. The physical parameters can not be the ones which define the theory through its Lagrangian (bare parameters) because once we consider the effects of interactions, the direct connection between physical and bare parameters breaks. The renormalization procedure deals with the need to express our results in terms of measured quantities rather than abstract parameters which appear in the Lagrangian. To make contact with reality, the Lagrangian can be written in terms of renormalized fields and parameters. The remaining terms, which relate renormalized and bare quantities, are reinterpreted as counterterms. It is worth to mention that the renormalization is not intrinsically related with the existence of infinities in the theory and it is a necessary procedure even if the theory is finite.

A widely-used scheme of renormalization is the modified minimal substraction scheme ($\overline{\text{MS}}$). In the $\overline{\text{MS}}$ renormalization scheme, the pole, the Euler-Mascheroni constant, γ_E, and the $\ln(4\pi)$ terms are associated with the counterterms.

The dimensional regularization and the $\overline{\text{MS}}$ renormalization scheme are widely used when account for the necessary elements to compute the magnetic correction to the neutral pion mass at one-loop.

Appendix B

Magnetic corrections to the effective potential

Consider the contribution from a single charged boson to the effective potential at one-loop order, given by [55]

$$V_b^1 = -\frac{i}{2}\int \frac{d^4k}{(2\pi)^4}\ln\left[-D_b^{-1}(k)\right], \tag{B.1}$$

which can also be written as [56]

$$V_b^1 = \frac{1}{2}\int dm_b^2 \int \frac{d^4k}{(2\pi)^4} iD_b(k). \tag{B.2}$$

Using the boson propagator expanded over Landau levels in Eq. (3.13), taking a Wick rotation $k_0 \to ik_4$, and using a Schwinger parameter, we get

$$V_b^1 = \int dm_b^2 \int \frac{d^4k_E}{(2\pi)^4}\int_0^\infty ds \sum_{n=0}^{\infty}(-1)^n e^{-\frac{k_\perp^2}{|q_bB|}} L_n^0\left(\frac{2k_\perp^2}{|q_bB|}\right) e^{-s[k_{E\parallel}^2+m_b^2+(2n+1)|q_bB|-i\epsilon]}. \tag{B.3}$$

Using the definitions

$$\begin{aligned} s_1 &= 2k_\perp^2/|q_bB|, \\ r_1 &= -e^{-2s|q_bB|}, \\ \alpha(k_{E\parallel}) &= k_{E\parallel}^2 + m_b^2 - i\epsilon, \end{aligned} \tag{B.4}$$

we write

$$V_b^1 = \int dm_b^2 \int \frac{d^4k_E}{(2\pi)^4}\int_0^\infty ds \sum_{n=0}^{\infty} r_1^n L_n^0\left(s_1\right) e^{-s[\alpha(k_{E\parallel})+|q_bB|]} e^{-\frac{k_\perp^2}{|q_bB|}}. \tag{B.5}$$

Using the generating function of Laguerre polynomials

$$\sum_{n=0}^{\infty} r_1^n L_n^0(s_1) = \frac{1}{1-r_1} e^{-\frac{r_1}{1-r_1}s_1}, \tag{B.6}$$

we have

$$V_b^1 = \int dm_b^2 \int_0^\infty ds\, \frac{e^{-s|q_bB|}}{1-r_1} I_\perp(s) I_\parallel(s), \tag{B.7}$$

where we define

$$
\begin{aligned}
I_{\perp}(s) &= \int \frac{d^2k_{\perp}}{(2\pi)^2} e^{-\frac{k_{\perp}^2}{|q_b B|}(1-2\eta_b(s))}, \\
I_{\parallel}(s) &= \mu^{4-d} \int \frac{d^{d-2}k_{E\parallel}}{(2\pi)^{d-2}} e^{-s\alpha(k_{E\parallel})}, \\
\eta_b(s) &= \frac{1}{e^{2|q_b B|s}+1}.
\end{aligned}
\tag{B.8}
$$

We can take $\epsilon \to 0$ and use dimensional regularization. Once we carry out the integration, $I_{\perp}(s)$ and $I_{\parallel}(s)$ can be written as

$$
\begin{aligned}
I_{\perp}(s) &= \frac{|q_b B|}{4\pi \tanh\left(|q_b B|s\right)}, \\
I_{\parallel}(s) &= \mu^{2\varepsilon} \frac{1}{(4\pi s)^{1-\varepsilon}} e^{-s m_b^2}.
\end{aligned}
\tag{B.9}
$$

Using the explicit expressions in Eq. (B.9), we get

$$
V_b^1 = \int dm_b^2 \int_0^{\infty} ds \, \frac{|q_b B|}{8\pi \sinh\left(|q_b B|s\right)} \frac{\mu^{2\varepsilon}}{(4\pi s)^{1-\varepsilon}} e^{-s m_b^2}.
\tag{B.10}
$$

By writing

$$
\frac{1}{\sinh\left(|q_b B|s\right)} = 2 \sum_{n=0}^{\infty} e^{-(2n+1)|q_b B|s},
\tag{B.11}
$$

we can perform the integration over ds such that

$$
V_b^1 = \frac{|q_b B|}{16\pi^2} \int dm_b^2 \, \left(\frac{4\pi\mu^2}{2|q_b B|}\right)^{\varepsilon} \Gamma(\varepsilon) \, \zeta\left(\varepsilon, \frac{1}{2} + \frac{m_b^2}{2|q_b B|}\right).
\tag{B.12}
$$

Considering an expansion in $\varepsilon \to 0$, we have

$$
\begin{aligned}
V_b^1 \;=\; & \frac{|q_b B|}{16\pi^2} \int dm_b^2 \left\{ \zeta\left(0, \frac{1}{2} + \frac{m_b^2}{2|q_b B|}\right) \left[\frac{1}{\varepsilon} - \gamma_E + \ln\left(4\pi\right)\right.\right. \\
+ \; & \left.\left. \ln\left(\frac{\mu^2}{2|q_b B|}\right)\right] + \zeta^{(1,0)}\left(0, \frac{1}{2} + \frac{m_b^2}{2|q_b B|}\right) \right\},
\end{aligned}
\tag{B.13}
$$

where $\zeta(s,c)$ is the Hurwitz zeta function and it is classically defined by the formula

$$
\zeta(s,c) \equiv \sum_{n=0}^{\infty} \frac{1}{(n+c)^s},
\tag{B.14}
$$

for $c > 0$ and $R[s] > 1$ (by analytic continuation to other $s \neq 1$), and

$$
\frac{d}{ds}\zeta(s,c)|_{s=0} = \zeta^{(1,0)}(0,c).
\tag{B.15}
$$

Using the following identities:

$$\begin{aligned}\zeta\left(0,c\right) &= \frac{1}{2}-c,\\ \zeta^{(1,0)}\left(0,c\right) &= \ln\left[(2\pi)^{-1/2}\,\Gamma\left(c\right)\right],\end{aligned} \tag{B.16}$$

we get

$$\begin{aligned}V_b^1 &= -\frac{1}{32\pi^2}\int dm_b^2\, m_b^2\left\{\frac{1}{\varepsilon}-\gamma_E+\ln\left(4\pi\right)+\ln\left(\frac{\mu^2}{2|q_bB|}\right)\right.\\ &- \left.\frac{2|q_bB|}{m_b^2}\ln\left[(2\pi)^{-1/2}\,\Gamma\left(\frac{1}{2}+\frac{m_b^2}{2|q_bB|}\right)\right]\right\}.\end{aligned} \tag{B.17}$$

Considering the $\overline{\text{MS}}$ renormalization scheme, we have

$$V_b^1=\frac{1}{32\pi^2}\int dm_b^2\, m_b^2\left\{\frac{2|q_bB|}{m_b^2}\ln\left[\Gamma\left(\frac{1}{2}+\frac{m_b^2}{2|q_bB|}\right)\right]-\frac{|q_bB|}{m_b^2}\ln\left(2\pi\right)-\ln\left(\frac{\mu^2}{2|q_bB|}\right)\right\}, \tag{B.18}$$

solving the integral for dm_b^2, we get the final result

$$V_b^1=\frac{1}{16\pi^2}\left[2|q_bB|^2\psi^{-2}\left(\frac{1}{2}+\frac{m_b^2}{2|q_bB|}\right)-\frac{1}{2}|q_bB|m_b^2\ln(2\pi)-\frac{m_b^4}{4}\ln\left(\frac{\mu^2}{2|q_bB|}\right)\right], \tag{B.19}$$

where $\psi^{-2}(x)$ is the polygamma function of the order of -2. In the context of the LSMq we have to consider the contribution of both charged pions such that the magnetic correction from bosons in this model can be written as

$$V_{\pi^+}^1+V_{\pi^-}^1=\frac{1}{8\pi^2}\left[2|eB|^2\psi^{-2}\left(\frac{1}{2}+\frac{m_0^2}{2|eB|}\right)-\frac{1}{2}|eB|m_0^2\ln(2\pi)-\frac{m_0^4}{4}\ln\left(\frac{\mu^2}{2|eB|}\right)\right]. \tag{B.20}$$

The magnetic corrections from the fermion contribution to the effective potential can be computed from [57]

$$V_f^1=iN_c\int\frac{d^4k}{(2\pi)^4}\text{Tr}\,\ln\left[S_f^{-1}(k)\right]. \tag{B.21}$$

In a similar fashion to the boson case, it can be shown that

$$V_f^1=-2iN_c\sum_{\sigma=\pm1}\int dm_f^2\int\frac{d^4k}{(2\pi)^4}\sum_{n=0}(-1)^n e^{-\frac{k_\perp^2}{|q_fB|}}\frac{L_n^0\left(\frac{2k_\perp^2}{|q_fB|}\right)}{k_\parallel^2-m_f^2-(2n+1+\sigma)|q_fB|+i\epsilon}, \tag{B.22}$$

where we consider the particle-antiparticle contributions and a sum over the polarizations with respect to the magnetic field direction, σ. Making a Wick rotation and considering a Schwinger proper time parametrization, we have

$$\begin{aligned}V_f^1 &= -2N_c\sum_{\sigma=\pm1}\int dm_f^2\int_0^\infty ds\int\frac{d^4k}{(2\pi)^4}\sum_{n=0}^{\infty}(-1)^n e^{-\frac{k_\perp^2}{|q_fB|}}\\ &\times\; L_n^0\left(\frac{2k_\perp^2}{|q_fB|}\right)e^{-s\left[k_{E\parallel}^2+m_f^2+(2n+1+\sigma)|q_fB|-i\epsilon\right]}.\end{aligned} \tag{B.23}$$

Using the following definitions:

$$\begin{aligned} s_2 &= 2k_\perp^2/|q_f B|, \\ r_2 &= -e^{-2s|q_f B|}, \\ \beta(k_{E\parallel}) &= k_{E\parallel}^2 + m_f^2 - i\epsilon, \end{aligned} \tag{B.24}$$

we get

$$V_f^1 = -2N_c \sum_{\sigma=\pm 1} \int dm_f^2 \int_0^\infty ds \int \frac{d^4k}{(2\pi)^4} \sum_{n=0}^\infty r_2^n L_n^0\left(s_2\right) e^{-s\left[\beta(k_{E\parallel}^2)+|q_f B|+\sigma|q_f B|\right]} e^{-\frac{k_\perp^2}{|q_f B|}}. \tag{B.25}$$

Using the generating function of Laguerre polynomials

$$\sum_{n=0}^\infty r_2^n L_n^0(s_2) = \frac{1}{1-r_2} e^{-\frac{r_2}{1-r_2}s_2}, \tag{B.26}$$

we obtain

$$V_f^1 = -2N_c \sum_{\sigma=\pm 1} \int dm_f^2 \int_0^\infty ds \int \frac{d^4k}{(2\pi)^4} \frac{e^{-s|q_f B|}}{1-r_2} e^{-s|q_f B|} J_\perp(s) J_\parallel(s), \tag{B.27}$$

where after introducing dimensional regularization, we use the definitions

$$\begin{aligned} J_\perp(s) &= \int \frac{d^2k_\perp}{(2\pi)^2} e^{-\frac{k_\perp^2}{|q_f B|}(1-2\eta_f(s))}, \\ J_\parallel(s) &= \mu^{4-d} \int \frac{d^{d-2}k_{E\parallel}}{(2\pi)^{d-2}} e^{-s\beta(k_{E\parallel})}, \\ \eta_f(s) &= \frac{1}{e^{2|q_f B|s}+1}, \end{aligned} \tag{B.28}$$

where we have considered $\epsilon \to 0$. Once we carry out the integration, $J_\perp(s)$ and $J_\parallel(s)$ can be written as

$$\begin{aligned} J_\perp(s) &= \frac{|q_f B|}{4\pi \tanh\left(|q_f B|s\right)}, \\ J_\parallel(s) &= \mu^{2\varepsilon} \frac{1}{(4\pi s)^{1-\varepsilon}} e^{-sm_f^2}. \end{aligned} \tag{B.29}$$

Using the identity

$$\sum_{\sigma=\pm 1} e^{-s|q_f B|} = 2\cosh\left(|q_f B|s\right), \tag{B.30}$$

we have

$$V_f^1 = -2N_c \int dm_f^2 \int_0^\infty ds \frac{|q_f B|}{4\pi \tanh\left(|q_f B|s\right)} \frac{\mu^{2\varepsilon}}{(4\pi s)^{1-\varepsilon}} e^{-sm_f^2}. \tag{B.31}$$

We now use that

$$\frac{1}{\tanh\left(|q_f B|s\right)} = \sum_{n=0}^\infty e^{-2n|q_f B|s} + \sum_{n=0}^\infty e^{-(2n+2)|q_f B|s}, \tag{B.32}$$

to integrate over ds such that

$$V_f^1 = -\frac{N_c|q_fB|}{8\pi^2}\int dm_f^2\left(\frac{4\pi\mu^2}{2|q_fB|}\right)^{\varepsilon}\Gamma(\varepsilon)\left[\zeta\left(\varepsilon,\frac{m_f^2}{2|q_fB|}\right)+\zeta\left(\varepsilon,\frac{m_f^2}{2|q_fB|}+1\right)\right]. \tag{B.33}$$

Considering an expansion in $\varepsilon\to 0$, we get

$$\begin{aligned} V_f^1 &= -\frac{N_c|q_fB|}{8\pi^2}\int dm_f^2\left\{\zeta^{(1,0)}\left(0,\frac{m_f^2}{2|q_fB|}\right)+\zeta^{(1,0)}\left(0,\frac{m_f^2}{2|q_fB|}+1\right)+\left[\zeta\left(0,\frac{m_f^2}{2|q_fB|}+1\right)\right.\right. \\ &+ \left.\left.\zeta\left(0,\frac{m_f^2}{2|q_fB|}\right)\right]\left[\frac{1}{\varepsilon}-\gamma_E+\ln(4\pi)+\ln\left(\frac{\mu^2}{2|q_fB|}\right)\right]\right\}. \end{aligned} \tag{B.34}$$

Using the identities in Eq. (B.16), we have

$$\begin{aligned} V_f^1 &= \frac{N_c}{8\pi^2}\int dm_f^2\, m_f^2\left\{\frac{1}{\varepsilon}-\gamma_E+\ln(4\pi)+\ln\left(\frac{\mu^2}{2|q_fB|}\right)-\frac{|q_fB|}{m_f^2}\ln\left(\frac{m_f^2}{2|q_fB|}\right)\right. \\ &- \left.\frac{2|q_fB|}{m_f^2}\ln\left[\Gamma\left(\frac{m_f^2}{2|q_fB|}\right)\right]+\frac{|q_fB|}{m_f^2}\ln(2\pi)\right\}. \end{aligned} \tag{B.35}$$

After the $\overline{\text{MS}}$ renormalization scheme is implemented, we get

$$\begin{aligned} V_f^1 &= -\frac{N_c}{8\pi^2}\int dm_f^2\left\{|q_fB|\ln\left(\frac{m_f^2}{2|q_fB|}\right)-|q_fB|\ln(2\pi)-m_f^2\ln\left(\frac{\mu^2}{2|q_fB|}\right)\right. \\ &+ \left.2|q_fB|\ln\left[\Gamma\left(\frac{m_f^2}{2|q_fB|}\right)\right]\right\}. \end{aligned} \tag{B.36}$$

Finally, integrating over dm_f^2, we obtain

$$\begin{aligned} V_f^1 &= -\frac{N_c}{8\pi^2}\left[4|q_fB|^2\psi^{-2}\left(\frac{m_f^2}{2|q_fB|}\right)-\frac{m_f^4}{2}\ln\left(\frac{\mu^2}{2|q_fB|}\right)-m_f^2|q_fB|-m_f^2|q_fB|\ln(2\pi)\right. \\ &+ \left.m_f^2|q_fB|\ln\left(\frac{m_f^2}{2|q_fB|}\right)\right]. \end{aligned} \tag{B.37}$$

Appendix C

Magnetic corrections to the neutral pion self-energy

Consider the quark loop which can be made either of quarks u or d, as depicted in Fig. 4.3. The contribution from a quark flavor f is given by

$$-i\Pi_{f\bar{f}}(B,q) = -g^2 \int \frac{d^4k}{(2\pi)^4} Tr[\gamma^5 iS_f(k)\gamma^5 iS_f(k+q)] + \text{CC}, \tag{C.1}$$

where we used that the Schwinger phase vanishes. We now use Eq. (3.17) to account for the strong field limit, and the properties of the Dirac matrices

$$\begin{aligned}
&\mathcal{O}^{\pm}\not{a}_{\parallel} = \not{a}_{\parallel}\mathcal{O}^{\pm},\\
&\mathcal{O}^{\pm}\gamma^5 = \gamma^5\mathcal{O}^{\pm},\\
&\mathcal{O}^{+} + \mathcal{O}^{-} = \mathbb{I},\\
&\left(\mathcal{O}^{\pm}\right)^2 = \mathcal{O}^{\pm},\\
&\gamma^5\not{a}_{\parallel} = -\not{a}_{\parallel}\gamma^5,
\end{aligned} \tag{C.2}$$

where $a^{\mu}_{\parallel} = (a_0, 0, 0, a_3)$, $\not{a}_{\parallel} = a_{\parallel\mu}\gamma^{\mu}$ and the projection operators are defined according to Eq. (3.16). Adding up the contribution from the CC diagram, we get

$$-i\Pi_{f\bar{f}} = 4g^2 \int \frac{d^4k}{(2\pi)^4} e^{-\frac{k_{\perp}^2 + (k+q)_{\perp}^2}{|q_f B|}} \frac{\mathcal{N}}{AB}, \tag{C.3}$$

where we define

$$\begin{aligned}
&\mathcal{N} \equiv Tr\left[(m_f - \not{k}_{\parallel})((\not{k} + \not{q})_{\parallel} + m_f)\right]\\
&A = (k+q)_{\parallel}^2 - m_f^2 + i\epsilon,\\
&B = k_{\parallel}^2 - m_f^2 + i\epsilon.
\end{aligned} \tag{C.4}$$

We proceed to integrate over the perpendicular coordinates relative to the magnetic field. The result is given by

$$-i\Pi_{f\bar{f}} = g^2 \frac{|q_f B|}{2\pi} e^{-\frac{1}{2|q_f B|}q_{\perp}^2} \int \frac{d^2k_{\parallel}}{(2\pi)^2} \frac{\mathcal{N}}{AB}. \tag{C.5}$$

We introduce the Feynman parametrization

$$\frac{1}{AB} = \int_0^1 \frac{dx}{\left[Ax + B(1-x)\right]^2}. \tag{C.6}$$

The denominator of Eq. (C.5) can be written as

$$Ax + B(1-x) = (k + xq_\parallel)^2 - \Delta_1 + i\epsilon, \tag{C.7}$$

where $\Delta_1 = x(x-1)q_\parallel^2 + m_f^2$ and $\epsilon \to 0$. We make the change of variables $k_\parallel = l_\parallel - xq_\parallel$ such that the numerator, $\mathcal{N}$, can be expressed as

$$\mathcal{N} = 4m_f^2 - 4l_\parallel^2 + 4x(1-x)q_\parallel^2. \tag{C.8}$$

Notice that we have taken into account that the trace of an odd number of Dirac matrices vanishes and that the linear term $l_\parallel$ will vanish in the integration. Thus, the contribution to the self-energy becomes

$$-i\Pi_{f\bar{f}} = \frac{2g^2|q_fB|}{\pi} e^{-\frac{1}{2|q_fB|}q_\perp^2} \int_0^1 dx \int \frac{d^2l_\parallel}{(2\pi)^2} \left[-\frac{l_\parallel^2}{(l_\parallel^2 - \Delta_1)^2} + \frac{x(1-x)q_\parallel^2 + m_f^2}{(l_\parallel^2 - \Delta_1)^2} \right]. \tag{C.9}$$

In order to find the integral over parallel coordinates relative to the magnetic field we proceed using the dimensional regularization relations in Eqs.(A.13) and (A.14)

$$-i\Pi_{f\bar{f}} = \frac{ig^2|q_fB|}{2\pi^2} e^{-\frac{1}{2|q_fB|}q_\perp^2} \int_0^1 dx \left[\frac{1}{\varepsilon} + \ln(4\pi) - \gamma_E - \ln\left(\frac{\Delta_1}{\mu^2}\right) - 1 + \frac{x(1-x)q_\parallel^2 + m_f^2}{\Delta_1} \right]. \tag{C.10}$$

In the static limit, $\vec{q} = \vec{0}$, and setting the zeroth component of the momentum equal to the neutral pion mass, $q_0 = m_B$, one can solve Eq. (5.1) self-consistently. We proceed using the $\overline{\text{MS}}$ renormalization scheme to obtain a finite expression given by

$$-i\Pi_{f\bar{f}} = \frac{ig^2|q_fB|}{2\pi^2} \int_0^1 dx \left[\frac{m_f^2 - x(x-1)m_B^2}{m_f^2 + x(x-1)m_B^2} - 1 - \ln\left(\frac{x(x-1)m_B^2 + m_f^2}{\mu^2}\right) \right]. \tag{C.11}$$

The integration over the Feynman parameter can be performed provided that $4m_f^2 > m_B^2$; this condition is the threshold relation for this process, and it must remain valid upon the choice of the set of parameters. Substituting and reducing terms, we get

$$\Pi_{f\bar{f}} = \frac{g^2|q_fB|}{2\pi^2} \left[\ln\left(\frac{m_f^2}{\mu^2}\right) - \frac{2m_B}{\sqrt{4m_f^2 - m_B^2}} \operatorname{arccsc}\left(\frac{2m_f}{m_B}\right) \right]. \tag{C.12}$$

Setting $\mu^2 = 2|eB| + m_0^2$, we obtain

$$\Pi_{f\bar{f}} = \frac{g^2|q_fB|}{2\pi^2} \left[\ln\left(\frac{m_f^2}{2|eB| + m_0^2}\right) - \frac{2m_B}{\sqrt{4m_f^2 - m_B^2}} \operatorname{arccsc}\left(\frac{2m_f}{m_B}\right) \right]. \tag{C.13}$$

Finally, we compute the contribution from the tadpole in Fig.4.4. Its explicit expression is given by

$$-i\Pi_{\pi^\pm} = \int \frac{d^4k}{(2\pi)^4} (-2i\lambda) iD_{\pi^\pm}(k), \tag{C.14}$$

where we used the fact that the Schwinger phase vanishes in the tadpole. In the strong field limit we use the boson propagator in Eq. (3.18). The contribution from the two charged pions can be written as

$$-i(\Pi_{\pi^+}+\Pi_{\pi^-}) = -8i\lambda \int \frac{d^4k}{(2\pi)^4} \frac{ie^{-\frac{k_\perp^2}{|eB|}}}{k_\parallel^2 - |eB| - m_0^2 + i\epsilon}. \tag{C.15}$$

We proceed with the integration over the perpendicular coordinates relative to the magnetic field to obtain

$$-i(\Pi_{\pi^+}+\Pi_{\pi^-}) = \frac{2\lambda|eB|}{\pi} \int \frac{d^2k_\parallel}{(2\pi)^2} \frac{1}{k_\parallel^2 - \Delta_2 + i\epsilon}, \tag{C.16}$$

where $\Delta_2 = |eB| + m_0^2$ and $\epsilon \to 0$. Using dimensional regularization as in Eq. (A.10), the integration over the parallel coordinates of momentum relative to the magnetic field direction can be found and taking $\varepsilon \to 0$, we have

$$-i(\Pi_{\pi^+}+\Pi_{\pi^-}) = -\frac{i\lambda|eB|}{2\pi^2}\left[\frac{1}{\varepsilon} + \ln(4\pi) - \gamma_E - \ln\left(\frac{|eB|+m_0^2}{\mu^2}\right)\right]. \tag{C.17}$$

Using the $\overline{\text{MS}}$ renormalization scheme, we obtain

$$\Pi_{\pi^+}+\Pi_{\pi^-} = -\frac{\lambda|eB|}{2\pi^2}\ln\left(\frac{|eB|+m_0^2}{\mu^2}\right). \tag{C.18}$$

Setting $\mu^2 = 2|eB| + m_0^2$, we get

$$\Pi_{\pi^+}+\Pi_{\pi^-} = -\frac{\lambda|eB|}{2\pi^2}\ln\left(\frac{|eB|+m_0^2}{2|eB|+m_0^2}\right). \tag{C.19}$$

Appendix D

Magnetic corrections to the boson self-coupling

To compute the magnetic correction to the boson self-coupling, we start from the Landau level representation of the charged boson propagator in Eq. (3.13) and use it with the expression for the magnetic correction to λ given by

$$-i6\lambda\Gamma^B_\lambda = \int \frac{d^4k}{(2\pi)^4}(-2i\lambda)iD^B_{\pi^-}(k)(-2i\lambda)iD^B_{\pi^-}(k+p+r) + \text{CC}. \tag{D.1}$$

Performing a Wick rotation in k and $s = r + p$, such that $k_0 \to ik_4$ and $s_0 \to is_4$, then

$$k^2_\parallel \to -k^2_{E\parallel},\ (k+s)^2_\parallel \to -(k+s)^2_{E\parallel},\ d^4k \to id^4k_E. \tag{D.2}$$

We now introduce two Schwinger parameters, $x_1,\ x_2$, $d^2x = dx_1dx_2$ such that the magnetic correction can be written as

$$\begin{aligned}\Gamma^B_\lambda &= -\frac{16}{3}\lambda\int\frac{d^4k_E}{(2\pi)^4}\int d^2x\sum_{n,m=0}^{\infty} r_1^n r_2^m L^0_n(s_1)\,L^0_m(s_2)\\ &\times\ e^{-\frac{k^2_\perp}{|q_bB|}-\frac{(k+s)^2_\perp}{|q_bB|}-x_1[\alpha(k_{E\parallel})+|q_bB|]-x_2[\beta(k_{E\parallel})+|q_bB|]},\end{aligned} \tag{D.3}$$

where

$$\begin{aligned}&s_1 = 2k^2_\perp/|q_bB|,\ s_2 = 2(k+s)^2_\perp/|q_bB|,\\ &\alpha(k_{E\parallel}) = k^2_{E\parallel}+m_0^2-i\epsilon,\\ &\beta(k_{E\parallel}) = (k+s)^2_{E\parallel}+m_0^2-i\epsilon,\end{aligned} \tag{D.4}$$

and $r_i = -e^{-2|q_bB|x_i}$, $i = 1, 2$. Using the generating function of Laguerre polynomials

$$\sum_{n=0}^{\infty} r_i^n L^0_n(s_i) = \frac{1}{1-r_i}e^{-\frac{r_i}{1-r_i}s_i}, \tag{D.5}$$

we obtain

$$\Gamma^B_\lambda = -\frac{16}{3}\lambda\int d^2x\frac{e^{-(x_1+x_2)|q_bB|}}{(1-r_1)(1-r_2)}I(x_1,x_2)J(x_1,x_2), \tag{D.6}$$

where we define

$$
\begin{aligned}
I(x_1,x_2) &= \int \frac{d^2k_\perp}{(2\pi)^2} e^{-\frac{k_\perp^2}{|q_bB|}(1-2\eta(x_1))-\frac{(k+s)_\perp^2}{|q_bB|}(1-2\eta(x_2))},\\
J(x_1,x_2) &= \mu^{4-d}\int \frac{d^{d-2}k_{E\parallel}}{(2\pi)^{d-2}} e^{-x_1\alpha(k_{E\parallel})-x_2\beta(k_{E\parallel})},\\
\eta(|q_bB|x_i) &= \frac{1}{e^{2|q_bB|x_i}+1},
\end{aligned}
\tag{D.7}
$$

with $i = 1, 2$ and $\epsilon \to 0$. To carry out the integrals, we use dimensional regularization, namely,

$$
\int \frac{d^4k_E}{(2\pi)^4} \to \mu^{4-d}\int \frac{d^{d-2}k_{E\parallel}}{(2\pi)^{d-2}}\int \frac{d^2k_\perp}{(2\pi)^2}. \tag{D.8}
$$

First, to find $I(x_1, x_2)$ we consider the change of variable

$$
q_\perp = k_\perp + \frac{1-2\eta(|q_bB|x_2)}{2(1-\eta(|q_bB|x_1)-\eta(|q_bB|x_2))}s_\perp, \tag{D.9}
$$

and the identity

$$
1-2\eta(|q_bB|x_i) = \tanh(|q_bB|x_i). \tag{D.10}
$$

Completing the square, we have

$$
\begin{aligned}
I(x_1,x_2) &= \frac{|q_bB|/4\pi}{\tanh(|q_bB|x_1)+\tanh(|q_bB|x_2)}\\
\times\quad &\exp\left[-\frac{\tanh(|q_bB|x_1)\tanh(|q_bB|x_2)}{|q_bB|(\tanh(|q_bB|x_1)+\tanh(|q_bB|x_2))}s_\perp^2\right].
\end{aligned}
\tag{D.11}
$$

Next, $J(x_1, x_2)$ can be found using the change of variables

$$
q_{E\parallel} = k_{E\parallel} + \frac{x_2}{x_1+x_2}s_{E\parallel}. \tag{D.12}
$$

Carrying out the integral and using $d = 4 - 2\varepsilon$, we obtain

$$
J(x_1,x_2) = \mu^{2\varepsilon}\left(\frac{1}{4\pi(x_1+x_2)}\right)^{1-\varepsilon} e^{-\frac{x_1x_2}{x_1+x_2}s_{E\parallel}^2-(x_1+x_2)m_0^2}. \tag{D.13}
$$

Using the identities

$$
\frac{e^{-x_i|q_bB|}}{1-r_i} = \frac{1}{2\cosh(|q_bB|x_i)}, \tag{D.14}
$$

and

$$
\frac{1}{\sinh(|q_bB|(x_1+x_2))} = \frac{1}{\tanh(|q_bB|x_1)+\tanh(|q_bB|x_2)}\frac{1}{\cosh(|q_bB|x_1)\cosh(|q_bB|x_2)}, \tag{D.15}
$$

together with Eqs. (D.11) and (D.13), we get

$$
\begin{aligned}
\Gamma_\lambda^B &= -\frac{\lambda}{12\pi^2}\int d^2x \frac{(4\pi\mu^2)^\varepsilon}{(x_1+x_2)^{1-\varepsilon}}\frac{|q_bB|}{\sinh(|q_bB|(x_1+x_2))}\exp\left[-\frac{x_1x_2}{x_1+x_2}s_{E\parallel}^2-(x_1+x_2)m_0^2\right]\\
&\times\quad \exp\left[-\frac{\tanh(|q_bB|x_1)\tanh(|q_bB|x_2)}{|q_bB|(\tanh(|q_bB|x_1)+\tanh(|q_bB|x_2))}s_\perp^2\right].
\end{aligned}
\tag{D.16}
$$

We perform the change of variables

$$x_1 = s(1-y), \quad x_2 = sy, \quad dx_1 dx_2 = sdsdy. \tag{D.17}$$

These variables have the domains $0 < y < 1$ and $s > 0$. Substituting these new variables, we obtain

$$\begin{aligned}\Gamma^B_\lambda &= -\frac{\lambda}{12\pi^2}\int_0^\infty ds \int_0^1 dy\, (4\pi\mu^2 s)^\varepsilon \frac{|q_b B|}{\sinh(|q_b B|s)} \exp\left[-sy(1-y)s^2_{E\parallel} - sm_0^2\right] \\ &\times \exp\left[-\frac{\tanh(|q_b B|s(1-y))\tanh(|q_b B|sy)}{|q_b B|(\tanh(|q_b B|s(1-y)) + \tanh(|q_b B|sy))} s^2_\perp\right].\end{aligned} \tag{D.18}$$

Equation (D.18) is the general expression for the magnetic correction to the boson self-coupling. This expression contains a divergence that should be regularized. Considering the static limit in Eq. (D.18), which implies that $s^2_{E\parallel} \to 0$ and $s^2_\perp = 0$, the general magnetic correction reduces to

$$\Gamma^B_\lambda = -\frac{\lambda}{12\pi^2}\int_0^\infty ds\, (4\pi\mu^2 s)^\varepsilon \frac{|q_b B|}{\sinh(|q_b B|s)} e^{-sm_0^2}. \tag{D.19}$$

Notice that in this limit both integrals can be solved analytically

$$\int_0^\infty ds \frac{s^\varepsilon e^{-sm_0^2}}{\sinh(|q_b B|s)} = \frac{1}{|q_b B|}\left(\frac{1}{2|q_b B|}\right)^\varepsilon \Gamma(\varepsilon+1)\zeta\left(\varepsilon+1, \frac{|q_b B| + m_0^2}{2|q_b B|}\right), \tag{D.20}$$

where ζ is the Hurwitz zeta function. Considering an expansion in $\varepsilon \to 0$, we have

$$\begin{aligned}&\left(\frac{4\pi\mu^2}{2|q_b B|}\right)^\varepsilon \approx 1 + \varepsilon \ln\left(\frac{4\pi\mu^2}{2|q_b B|}\right), \\ &\Gamma(\varepsilon+1) \approx 1 - \varepsilon\gamma_E, \\ &\zeta\left(\varepsilon+1, \frac{|q_b B| + m_0^2}{2|q_b B|}\right) \approx \frac{1}{\varepsilon} - \psi^0\left(\frac{|q_b B| + m_0^2}{2|q_b B|}\right),\end{aligned} \tag{D.21}$$

where ψ^0 is the digamma function. Therefore, we finally obtain

$$\begin{aligned}\Gamma^B_\lambda &= -\frac{\lambda}{12\pi^2}\left[\frac{1}{\varepsilon} - \gamma_E + \ln(4\pi) - \psi^0\left(\frac{|q_b B| + m_0^2}{2|q_b B|}\right)\right. \\ &+ \left.\ln\left(\frac{\mu^2}{2|q_b B|}\right)\right],\end{aligned} \tag{D.22}$$

where $|q_b B| = |eB|$.

Finally, the magnetic correction to the λ coupling in strong field limit can be determined using the Eq. (D.1)

$$-i6\lambda\Gamma^{LLL}_\lambda = \int \frac{d^4k}{(2\pi)^4}(-2i\lambda)D^{LLL}_{\pi^-}(k)(-2i\lambda)D^{LLL}_{\pi^-}(k+p+r) + \text{CC}, \tag{D.23}$$

writing explicitly the charged scalar propagator in the LLL approximation and considering a two factor from the charged conjugate diagram, we get

$$\Gamma^{LLL}_\lambda = -\frac{4}{3}i\lambda\int \frac{d^4k}{(2\pi)^4}\frac{2ie^{-\frac{k^2_\perp}{|eB|}}}{k^2_\parallel - |eB| - m_0^2 + i\epsilon}\frac{2ie^{-\frac{(k+p+r)^2_\perp}{|eB|}}}{(k+p+r)^2_\parallel - |eB| - m_0^2 + i\epsilon}, \tag{D.24}$$

let us denote $s \equiv p + r$ and doing the integral in the perpendicular as follows

$$\int \frac{d^2k_\perp}{(2\pi)^2} e^{-\frac{k_\perp^2}{|eB|}} e^{-\frac{(k+p+r)_\perp^2}{|eB|}} = \frac{|eB|}{8\pi} e^{-\frac{1}{2|eB|}s_\perp^2}, \tag{D.25}$$

substituting the last result, we obtain

$$\Gamma_\lambda^{LLL} = \frac{2}{3\pi} i\lambda |eB| e^{-\frac{s_\perp^2}{2|eB|}} \int \frac{d^2k_\parallel}{(2\pi)^2} \frac{1}{k_\parallel^2 - |eB| - m_0^2 + i\epsilon} \frac{1}{(k+s)_\parallel^2 - |eB| - m_0^2 + i\epsilon}. \tag{D.26}$$

In order to integrate the parallel coordinates we use a Feynman parameter

$$\Gamma_\lambda^{LLL} = \frac{2}{3\pi} i\lambda |eB| e^{-\frac{s_\perp^2}{2|eB|}} \int_0^1 dx \int \frac{d^2k_\parallel}{(2\pi)^2} \frac{1}{[Cx + D(1-x)]^2},$$

where $C = (k+s)_\parallel^2 - |eB| - m_0^2 + i\epsilon$ y $D = k_\parallel^2 - |eB| - m_0^2 + i\epsilon$. Considering a change of variable in the denominator such as $k_\parallel = q_\parallel - xs_\parallel$, $d^2k_\parallel = d^2q_\parallel$ and $\Delta_3 = x(x-1)s_\parallel^2 + |eB| + m_0^2$, we have

$$\Gamma_\lambda^{LLL} = \frac{2}{3\pi} i\lambda |eB| e^{-\frac{s_\perp^2}{2|eB|}} \int_0^1 dx \int \frac{d^2q_\parallel}{(2\pi)^2} \frac{1}{(q_\parallel^2 - \Delta_3 + i\epsilon)^2},$$

Setting $\epsilon \to 0$ and using the equation (A.13) in order to perform the dimensional regularization, we have

$$\Gamma_\lambda^{LLL} = -\frac{1}{6\pi^2} \lambda |eB| e^{-\frac{s_\perp^2}{2|eB|}} \int_0^1 dx \, \frac{1}{\Delta},$$

substituting the value of Δ

$$\Gamma_\lambda^{LLL} = -\frac{1}{6\pi^2} \lambda |eB| e^{-\frac{s_\perp^2}{2|eB|}} \int_0^1 dx \, \frac{1}{x(x-1)s_\parallel^2 + |eB| + m_0^2}. \tag{D.27}$$

Considering the static limit $p_0 = r_0 = m_0$ and $\vec{p} = \vec{r} = \vec{0}$

$$\Gamma_\lambda^{LLL} = -\frac{1}{6\pi^2} \lambda |eB| e^{-\frac{s_\perp^2}{2|eB|}} \int_0^1 dx \, \frac{1}{4m_0^2 x(x-1) + |eB| + m_0^2},$$

we can use the following relation to integrate over the Feynman parameter

$$\int_0^1 dx \, \frac{1}{4x(x-1) + a} = \frac{1}{\sqrt{a-1}} \arctan\left(\frac{1}{\sqrt{a-1}}\right), \quad a > 1,$$

taking $a = (|eB| + m_0^2)/m_0^2$ which satisfies the required condition, we get

$$\Gamma_\lambda^{LLL} = -\frac{1}{6\pi^2} \lambda \frac{\sqrt{|eB|}}{m_0} \arctan\left(\frac{m_0}{\sqrt{|eB|}}\right). \tag{D.28}$$

Another case of interest is to consider all component of external momentum as zero, this assumption let us obtain the following expression

$$\Gamma_\lambda^{LLL} = -\frac{1}{6\pi^2} \lambda \frac{|eB|}{|eB| + m_0^2}. \tag{D.29}$$

Appendix E

Magnetic corrections to the boson-fermion coupling

We start writing the contribution from the diagram in Fig. 4.7(a) which can be obtained from the expression

$$
\begin{aligned}
I^B_{1,g} &= \int d^4x\, d^4y\, d^4x \int \frac{d^4s}{(2\pi)^4}\frac{d^4t}{(2\pi)^4}\frac{d^4k}{(2\pi)^4}\, e^{i\Phi_{1,l}} e^{-ip\cdot y}\left(\sqrt{2}g\gamma^5\right) e^{-is\cdot(x-y)} iS_d(s)\left(-g\gamma^5\right) e^{iq\cdot x} \\
&\times\ e^{-it\cdot(z-x)} iS_d(t)\left(\sqrt{2}g\gamma^5\right) e^{-ik\cdot(y-z)} iD_{\pi^-}(k) e^{ir\cdot z} + \text{CC},
\end{aligned}
\tag{E.1}
$$

where the Schwinger phase contribution is finite and is given by

$$
\Phi_{1,l} = \frac{1}{2}|eB|\varepsilon_{ij}\left(x_i y_j + y_i z_j + z_i x_j\right), \quad i,j = 1,2. \tag{E.2}
$$

The integration over configuration space can be performed using the factorization between parallel and perpendicular components. Recall that for four-vectors a_μ and b_μ

$$
a_\mu b^\mu = a_0 b_0 - a_1 b_1 - a_2 b_2 - a_3 b_3 = a_\parallel \cdot b_\parallel - a_\perp \cdot b_\perp. \tag{E.3}
$$

Thus, integrating over configuration space and taking into account Eq. (E.3) to include the Schwinger phase contribution, we obtain

$$
\begin{aligned}
I^B_{1,g} &= \delta^{(2)}(p-q-r)_\perp \int \frac{d^4s}{(2\pi)^4}\frac{d^4t}{(2\pi)^4}\frac{d^4k}{(2\pi)^4}\,\frac{4}{|eB|^2}(2\pi)^{10}\delta^{(2)}(s-q-t)_\parallel \\
&\times\ \delta^{(2)}(p-s+k)_\parallel \left(\sqrt{2}g\gamma^5\right) iS_d(s)\left(-g\gamma^5\right) iS_d(t)\left(\sqrt{2}g\gamma^5\right) iD_{\pi^-}(k) \\
&\times\ e^{i\frac{2}{|eB|}\varepsilon_{ij}(s-q-t)_i(s-p-k)_j} + \text{CC}.
\end{aligned}
\tag{E.4}
$$

We first integrate over $d^2s_\parallel$ and $d^2t_\parallel$ using the Dirac delta distributions to get

$$
\begin{aligned}
I^B_{1,g} &= (2\pi)^4\delta^{(4)}(p-q-r)\frac{1}{\pi^2|eB|^2}\int d^2s_\perp d^2t_\perp \frac{d^4k}{(2\pi)^4}\left(\sqrt{2}g\gamma^5\right) iS_d(k_\parallel + p_\parallel, s_\perp)\left(-g\gamma^5\right) \\
&\times\ iS_d(k_\parallel + r_\parallel, t_\perp)\left(\sqrt{2}g\gamma^5\right) iD_{\pi^-}(k_\parallel, k_\perp) e^{i\frac{2}{|eB|}\varepsilon_{ij}(s-q-t)_i(s-p-k)_j} + \text{CC}.
\end{aligned}
\tag{E.5}
$$

Notice that with this procedure we can identify the Dirac delta distribution for energy-momentum conservation in Eq. (E.5) such that

$$I^B_{1,g} = (2\pi)^4\delta^{(4)}(p-r-q)g\gamma^5\Gamma^B_{1,g}. \tag{E.6}$$

The contribution to the magnetic correction to the boson-fermion coupling, $g\gamma^5\Gamma^B_{1,g}$, is thus given by

$$\begin{aligned} g\gamma^5\Gamma^B_{1,g} &= \int \frac{d^2s_\perp d^2t_\perp}{\pi^2|eB|^2}\frac{d^4k}{(2\pi)^4}\left(\sqrt{2}g\gamma^5\right) iS_d(k_\parallel+p_\parallel,s_\perp)\left(-g\gamma^5\right) iS_d(k_\parallel+r_\parallel,t_\perp) \\ &\times \left(\sqrt{2}g\gamma^5\right) iD_{\pi^-}(k_\parallel,k_\perp)e^{i\frac{2}{|eB|}\varepsilon_{ij}(s-q-t)_i(s-p-k)_j} + \text{CC}. \end{aligned} \tag{E.7}$$

Equation (E.7) is general enough and could be computed using either the complete propagators or approximations to them. In this work we consider the propagators in the strong field limit. Substituting Eqs. (3.18) and (3.17) and adding the charge conjugate contribution, we have

$$\Gamma^{LLL}_{1,g} = \frac{16ig^2}{\pi^2|eB|^2}\int d^2s_\perp d^2t_\perp \frac{d^4k}{(2\pi)^4} e^{-\frac{s_\perp^2}{|q_dB|}-\frac{t_\perp^2}{|q_dB|}-\frac{k_\perp^2}{|q_{\pi^-}B|}}\frac{\mathcal{N}_1}{A_1B_1C_1}\, e^{i\frac{2}{|eB|}\varepsilon_{ij}(s-q-t)_i(s-p-k)_j}, \tag{E.8}$$

where we have defined for convenience the quantities

$$\begin{aligned} \mathcal{N}_1 &= (\not{k}_\parallel + \not{p}_\parallel + m_d)(m_d - \not{k}_\parallel - \not{r}_\parallel), \\ A_1 &= (k_\parallel + p_\parallel)^2 - m_d^2 + i\epsilon, \\ B_1 &= (k_\parallel + r_\parallel)^2 - m_d^2 + i\epsilon, \\ C_1 &= k_\parallel^2 - m_0^2 - |eB| + i\epsilon. \end{aligned} \tag{E.9}$$

We also resort to working in the static limit, setting the perpendicular coordinates of external momenta to zero. On doing so, we can integrate over the perpendicular coordinates relative to the magnetic field. The result is given by

$$\Gamma^{LLL}_{1,g} = \frac{ig^2|eB|}{4\pi}\int \frac{d^2k_\parallel}{(2\pi)^2}\frac{\mathcal{N}_1}{A_1B_1C_1}, \tag{E.10}$$

Introducing the Feynman parametrization

$$\frac{1}{A_1B_1C_1} = \int_0^1 dx \int_0^{1-x} \frac{2dy}{(A_1x + B_1y + C_1(1-x-y))^3}. \tag{E.11}$$

The denominator of Eq. (E.11) can be expressed as

$$A_1x + B_1y + C_1(1-x-y) = (k_\parallel + xp_\parallel + yr_\parallel)^2 - \Delta + i\epsilon, \tag{E.12}$$

where

$$\begin{aligned} \Delta &= (xp_\parallel + yr_\parallel)^2 - xp_\parallel^2 + xm_d^2 - yr_\parallel^2 + ym_d^2 \\ &+ (1-x-y)(m_0^2 + |eB|). \end{aligned} \tag{E.13}$$

On the other hand, it is useful to consider the change of variables as $k_\parallel = l_\parallel - xp_\parallel - yr_\parallel$, $dk_\parallel = dl_\parallel$. Then the numerator, $\mathcal{N}$, can be written as

$$\begin{aligned}\mathcal{N}_1 &= -l_\parallel^2 - 2xyp_\parallel \cdot r_\parallel + m_d \not{p}_\parallel - m_d \not{r}_\parallel - x(x-1)p_\parallel^2 \\ &- y(y-1)r_\parallel^2 - (1-x-y)\not{p}_\parallel \not{r}_\parallel + m_d^2,\end{aligned} \tag{E.14}$$

where we have already discarded linear terms of $l_\parallel$. At this point we can use the Dirac equation for outgoing states assuming that they are not affected by the external magnetic field. This means that the spinors satisfy the Dirac equation in vacuum

$$\bar{u}(p_\parallel)\not{p}_\parallel = \bar{u}(p_\parallel)m_u, \quad \not{r}_\parallel u(r_\parallel) = m_u u(r_\parallel). \tag{E.15}$$

Here, it is worth to note that in this computation we assume that the values of the quark masses remain fixed to just their vacuum values, $m_d = m_u = m_f$. Then, taking the static limit, $p_3 = r_3 = 0$ and $p_0 = r_0 = m_f$, we get

$$\bar{u}(p_\parallel)\mathcal{N}_1 u(r_\parallel) = \bar{u}(p_\parallel)(-l_\parallel^2 + 2m_f^2(x+y) - m_f^2(x+y)^2)u(r_\parallel). \tag{E.16}$$

Thus, once we consider $\bar{u}(p_\parallel)\Gamma_{1,g}^{LLL}u(r_\parallel)$ and use Eq. (E.16), we get

$$\Gamma_{1,g}^{LLL} = \frac{ig^2|eB|}{2\pi}\int_0^1 dx \int_0^{1-x} dy \int \frac{d^2l_\parallel}{(2\pi)^2}\left[\frac{-l_\parallel^2}{(l_\parallel^2 - \Delta + i\epsilon)^3} + \frac{2m_f^2(x+y) - m_f^2(x+y)^2}{(l_\parallel^2 - \Delta + i\epsilon)^3}\right], \tag{E.17}$$

where with the above assumptions, Δ is simplified to

$$\Delta = m_f^2(x+y)^2 + (1-(x+y))(m_0^2 + |eB|). \tag{E.18}$$

In order to integrate over $d^2l_\parallel$ we consider Eqs.(A.15) and (A.16), then

$$\Gamma_{1,g}^{LLL} = \frac{g^2|eB|}{16\pi^2 m_f^2}\int_0^1 dx \int_0^{1-x} dy \frac{1}{(x+y)^2 + \alpha(1-(x+y))}\left[1 + \frac{2(x+y) - (x+y)^2}{(x+y)^2 + \alpha(1-(x+y))}\right], \tag{E.19}$$

where $\alpha = (m_0^2 + |eB|)/m_f^2$. With the purpose of finding the integral over Feynman parameters, consider the following linear transformation

$$u = x + y, \quad v = 1 - x. \tag{E.20}$$

The Jacobian satisfies $det(J) = 1$ and the region of integration becomes $u \in [0,1]$ and $v \in [1-u, 1]$. Thus,

$$\Gamma_{1,g}^{LLL} = \frac{g^2|eB|}{16\pi^2 m_f^2}\int_0^1 du \int_{1-u}^1 dv \frac{1}{u^2 + \alpha(1-u)}\left[1 + \frac{(2-u)u}{u^2 + \alpha(1-u)}\right]. \tag{E.21}$$

Performing the integration over dv, we get the final expression for this contribution

$$\Gamma_{1,g}^{LLL} = \frac{g^2|eB|}{16\pi^2 m_f^2}\int_0^1 du \frac{u}{u^2 + \alpha(1-u)}\left[1 + \frac{(2-u)u}{u^2 + \alpha(1-u)}\right]. \tag{E.22}$$

We now proceed with $I_{2,g}$ which is given by

$$\begin{aligned} I^B_{2,g} &= \int d^4x\, d^4y\, d^4z \int \frac{d^4s}{(2\pi)^4}\frac{d^4t}{(2\pi)^4}\frac{d^4k}{(2\pi)^4} e^{i\Phi_{2,l}} e^{-ip\cdot y}\left(g\gamma^5\right) e^{-is\cdot(x-y)} iS_u(s)\left(g\gamma^5\right) e^{iq\cdot x} \\ &\times\ e^{-it\cdot(z-x)} iS_u(t)\left(g\gamma^5\right) e^{-ik\cdot(y-z)} iD_{\pi^0}(k) e^{ir\cdot z} + \text{CC}. \end{aligned} \tag{E.23}$$

Performing the integration over configuration space, we have

$$\begin{aligned} I^B_{2,g} &= \int \frac{d^4s}{(2\pi)^4}\frac{d^4t}{(2\pi)^4}\frac{d^4k}{(2\pi)^4} (2\pi)^{12}\delta^{(4)}(s-t-q)\delta^{(4)}(p-s+k)\delta^{(4)}(t-k-r)\left(g\gamma^5\right) \\ &\times\ iS_u(s)\left(g\gamma^5\right) iS_u(t)\left(g\gamma^5\right) iD_{\pi^0}(k) + \text{CC}, \end{aligned} \tag{E.24}$$

Integrating over d^4s and d^4t, we obtain

$$I^B_{2,g} = (2\pi)^4\delta^{(4)}(p-r-q)\int \frac{d^4k}{(2\pi)^4}\left(g\gamma^5\right) iS_u(k+p)\left(g\gamma^5\right) iS_u(k+r)\left(g\gamma^5\right) iD_{\pi^0}(k) + \text{CC}. \tag{E.25}$$

At this point we can identify the contribution to the magnetic correction from this diagram, $g\gamma^5\Gamma^B_{2,g}$, which can be expressed as

$$I^B_{2,g} = (2\pi)^4\delta^{(4)}(p-r-q) g\gamma^5\Gamma^B_{2,g}, \tag{E.26}$$

where

$$g\gamma^5\Gamma^B_{2,g} = \int \frac{d^4k}{(2\pi)^4}\left(g\gamma^5\right) iS_u(k+p)\left(g\gamma^5\right) iS_u(k+r)\left(g\gamma^5\right) iD_{\pi^0}(k) + \text{CC}. \tag{E.27}$$

Using Eqs. (3.17) and (3.18) to account for the strong field limit, we have

$$\Gamma^{LLL}_{2,g} = -4ig^2\int \frac{d^4k}{(2\pi)^4} e^{-\frac{(k+p)^2_\perp}{|q_uB|}-\frac{(k+r)^2_\perp}{|q_uB|}}\frac{\mathcal{N}_2}{A_2B_2C_2}, \tag{E.28}$$

where we define

$$\begin{aligned} \mathcal{N}_2 &= (\not{k}_\parallel + \not{p}_\parallel + m_u)(m_u - \not{k}_\parallel + \not{r}_\parallel), \\ A_2 &= (k_\parallel + p_\parallel)^2 - m_u^2 + i\epsilon, \\ B_2 &= (k_\parallel + r_\parallel)^2 - m_u^2 + i\epsilon, \\ C_2 &= k^2 - m_0^2 + i\epsilon. \end{aligned} \tag{E.29}$$

We now introduce a Feynman parametrization in the same fashion of Eq. (E.11). The denominator can be written as

$$A_2x + B_2y + C_2(1-x-y) = (k_\parallel + xp_\parallel + yr_\parallel)^2 - \Delta_\perp + i\epsilon, \tag{E.30}$$

where

$$\Delta_\perp = (xp_\parallel + yr_\parallel)^2 - xp_\parallel^2 + (x+y)m_u^2 - yr_\parallel^2 + (1-x-y)(m_0^2 + k_\perp^2). \tag{E.31}$$

Let us consider the change of variable $k_\parallel = l_\parallel - xp_\parallel - yr_\parallel$, $dk_\parallel = dl_\parallel$, then in terms of these variables, the numerator $\mathcal{N}_2$ can be written as

$$\begin{aligned}\mathcal{N}_2 &= -l_\parallel^2 - 2xyp_\parallel\cdot r_\parallel + m_u\not{p}_\parallel - m_u\not{r}_\parallel - x(x-1)p_\parallel^2 \\ &- y(y-1)r_\parallel^2 - (1-x-y)\not{p}_\parallel\not{r}_\parallel + m_u^2,\end{aligned} \tag{E.32}$$

where we already discarded linear terms in $l_\parallel$. We now use the Dirac equation for outgoing states once we set $p_i = r_i = 0$, $i = 1, 2$ and assume that these states are not affected by the external magnetic field, according to Eq. (E.15). Finally, setting $p_3 = r_3 = 0$ and $p_0 = r_0 = m_u$, we get

$$\bar{u}(p_\parallel)\mathcal{N}_2 u(r_\parallel) = \bar{u}(p_\parallel)(-l_\parallel^2 + 2m_u^2(x+y) - m_u^2(x+y)^2)u(r_\parallel). \tag{E.33}$$

Thus, once we have considered $\bar{u}(p_\parallel)\Gamma_{2,g}^{LLL}u(r_\parallel)$, we have

$$\begin{aligned}\Gamma_{2,g}^{LLL} &= -8ig^2\int_0^1 dx\int_0^{1-x} dy\int \frac{d^2k_\perp d^2l_\parallel}{(2\pi)^4}e^{-\frac{2k_\perp^2}{|q_uB|}} \\ &\times \left[\frac{-l_\parallel^2}{(l_\parallel^2 - \Delta_\perp + i\epsilon)^3} + \frac{2m_u^2(x+y) - m_u^2(x+y)^2}{(l_\parallel^2 - \Delta_\perp + i\epsilon)^3}\right],\end{aligned} \tag{E.34}$$

where $\Delta_\perp$ is simplified according to the previous assumptions to become

$$\Delta_\perp = m_u^2(x+y)^2 + (1-(x+y))(k_\perp^2 + m_0^2). \tag{E.35}$$

The integral over $d^2l_\parallel$ is found to be

$$\Gamma_{2,g}^{LLL} = -\frac{g^2}{\pi}\int_0^1 dx\int_0^{1-x} dy\int \frac{d^2k_\perp}{(2\pi)^2}e^{-\frac{2k_\perp^2}{|q_uB|}}\left[\frac{1}{\Delta_\perp} + \frac{2m_u^2(x+y) - m_u^2(x+y)^2}{\Delta_\perp^2}\right]. \tag{E.36}$$

Using the change of variables given in Eq. (E.20) the integral over dv can be performed to get

$$\Gamma_{2,g}^{LLL} = -\frac{g^2}{\pi m_u^2}\int_0^1 du\int \frac{d^2k_\perp}{(2\pi)^2}e^{-\frac{2k_\perp^2}{|q_uB|}}\frac{u}{u^2+\beta(1-u)}\left[1 + \frac{(2-u)u}{u^2+\beta(1-u)}\right], \tag{E.37}$$

where $\beta = (k_\perp^2 + m_0^2)/m_u^2$. We write the integration using polar coordinates

$$d^2k_\perp = dk_1dk_2 = k_\perp dk_\perp d\theta, \tag{E.38}$$

where $k_\perp = \sqrt{k_1^2 + k_2^2}$ and $\theta \in [0, 2\pi]$. Performing the integral over $d\theta$ and substituting $|q_uB| = 2|eB|/3$ and $m_u = m_f$, we have

$$\Gamma_{2,g}^{LLL} = -\frac{g^2}{2\pi^2 m_f^2}\int_0^1 du\int_0^\infty dk_\perp\, k_\perp e^{-\frac{3k_\perp^2}{|eB|}}\frac{u}{u^2+\beta(1-u)}\left[1 + \frac{(2-u)u}{u^2+\beta(1-u)}\right]. \tag{E.39}$$

Finally, $I_{3,g}^B$ can be written as

$$\begin{aligned}I_{3,g}^B &= \int d^4x\, d^4y\, d^4z\int \frac{d^4s}{(2\pi)^4}\frac{d^4t}{(2\pi)^4}\frac{d^4k}{(2\pi)^4}e^{i\Phi_{3,l}}e^{-ip\cdot y}\,(-ig)\,e^{-is\cdot(x-y)}iS_u(s)\left(g\gamma^5\right)e^{iq\cdot x} \\ &\times e^{-it\cdot(z-x)}iS_u(t)\,(-ig)\,e^{-ik\cdot(y-z)}iD_\sigma(k)e^{ir\cdot z} + \text{CC}.\end{aligned} \tag{E.40}$$

After integration over configuration space, we get

$$\begin{aligned} I^B_{3,g} &= \int \frac{d^4s}{(2\pi)^4}\frac{d^4t}{(2\pi)^4}\frac{d^4k}{(2\pi)^4}(2\pi)^{12}\delta^{(4)}(s-t-q)\delta^{(4)}(p-s+k)\delta^{(4)}(t-k-r)\,(-ig) \\ &\times\; iS_u(s)\left(g\gamma^5\right)iS_u(t)\,(-ig)\,iD_\sigma(k)+\text{CC}. \end{aligned} \tag{E.41}$$

Integrating over d^4s and d^4t, we have

$$I^B_{3,g} = (2\pi)^4\delta^{(4)}(p-q-r)\int \frac{d^4k}{(2\pi)^4}\,(-ig)\,iS_u(k+p)\left(g\gamma^5\right)iS_u(k+r)\,(-ig)\,iD_\sigma(k)+\text{CC}, \tag{E.42}$$

from where we can identify the contribution to the magnetic correction according to the expression

$$I^B_{3,g} = (2\pi)^4\delta^{(4)}(p-r-q)g\gamma^5\Gamma_{3,g}, \tag{E.43}$$

where

$$g\gamma^5\Gamma^B_{3,g} = \int \frac{d^4k}{(2\pi)^4}\,(-ig)\,iS_u(k+p)\left(g\gamma^5\right)iS_u(k+r)\,(-ig)\,iD_\sigma(k)+\text{CC}. \tag{E.44}$$

We now use the propagators for the charged particles in the LLL. After simplifying and adding the contribution from the charge conjugate diagram, we get

$$\Gamma^{LLL}_{3,g} = 4ig^2\int \frac{d^4k}{(2\pi)^4}e^{-\frac{(k+p)^2_\perp}{|q_uB|}-\frac{(k+r)^2_\perp}{|q_uB|}}\frac{\mathcal{N}_3}{A_3B_3C_3}, \tag{E.45}$$

where we define

$$\begin{aligned} \mathcal{N}_3 &= (m_u - \not{k}_\parallel - \not{p}_\parallel)(\not{k}_\parallel + \not{r}_\parallel + m_u), \\ A_3 &= (k_\parallel + p_\parallel)^2 - m_u^2 + i\epsilon, \\ B_3 &= (k_\parallel + r_\parallel)^2 - m_u^2 + i\epsilon, \\ C_3 &= k^2 - m_\sigma^2 + i\epsilon. \end{aligned} \tag{E.46}$$

The denominator can be written as

$$A_3x + B_3y + C_3(1-x-y) = (k_\parallel + xp_\parallel + yr_\parallel)^2 - \Delta_\perp + i\epsilon, \tag{E.47}$$

where

$$\Delta_\perp = (xp_\parallel + yr_\parallel)^2 - xp_\parallel^2 + (x+y)m_u^2 - yr_\parallel^2 + (1-x-y)(m_\sigma^2 + k_\perp^2). \tag{E.48}$$

Using the change of variable $k_\parallel = l_\parallel - xp_\parallel - yr_\parallel$, $dk_\parallel = dl_\parallel$, the numerator, $\mathcal{N}_3$, can be written as

$$\begin{aligned} \mathcal{N}_3 &= -l_\parallel^2 - 2xyp_\parallel\cdot r_\parallel - m_u\not{p}_\parallel + m_u\not{r}_\parallel - x(x-1)p_\parallel^2 \\ &- y(y-1)r_\parallel^2 - (1-x-y)\not{p}_\parallel\not{r}_\parallel + m_u^2, \end{aligned} \tag{E.49}$$

where we have neglected linear terms of $l_\parallel$. We proceed as for the previous cases. We use Eq. (E.15) and work in the static limit, $\vec{p} = \vec{r} = \vec{0}$ and $p_0 = r_0 = m_u$, to obtain

$$\bar{u}(p_\parallel)\mathcal{N}_3u(r_\parallel) = \bar{u}(p_\parallel)(-l_\parallel^2 + 2m_u^2(x+y) - m_u^2(x+y)^2)u(r_\parallel). \tag{E.50}$$

Thus, the integral can be written as

$$\Gamma_{3,g}^{LLL} = 8ig^2 \int \frac{d^2k_\perp}{(2\pi)^2} \int_0^1 dx \int_0^{1-x} dy \int \frac{d^2l_\parallel}{(2\pi)^2}\, e^{-\frac{2k_\perp^2}{|q_u B|}} \times \left[\frac{-l_\parallel^2}{(l_\parallel^2 - \Delta_\perp + i\epsilon)^3} + \frac{2m_u^2(x+y) - m_u^2(x+y)^2}{(l_\parallel^2 - \Delta_\perp + i\epsilon)^3} \right], \tag{E.51}$$

where

$$\Delta_\perp = m_u^2(x+y)^2 + (1-(x+y))(k_\perp^2 + m_\sigma^2). \tag{E.52}$$

Now, we can perform the integration over $d^2l_\parallel$ to get

$$\Gamma_{3,g}^{LLL} = \frac{g^2}{0} \int \frac{d^2k_\perp}{(2\pi)^2} \int_0^1 dx \int_0^{1-x} dy e^{-\frac{2k_\perp^2}{|q_u B|}} \left[\frac{1}{\Delta_\perp} + \frac{2m_u^2(x+y) - m_u^2(x+y)^2}{\Delta_\perp^2} \right]. \tag{E.53}$$

The last expression can be simplified if we consider the change of variables given by Eq. (E.20). After integration over dv, we have

$$\Gamma_{3,g}^{LLL} = \frac{g^2}{\pi m_u^2} \int_0^1 du \int \frac{d^2k_\perp}{(2\pi)^2}\, e^{-\frac{2k_\perp^2}{|q_u B|}} \frac{u}{u^2 + \gamma(1-u)} \left[1 + \frac{(2-u)u}{u^2 + \gamma(1-u)} \right], \tag{E.54}$$

where $\gamma = (k_\perp^2 + m_\sigma^2)/m_u^2$. We can now perform another integration after switching to polar coordinates according to Eq. (E.38). Performing the integration for $d\theta$ and substituting $|q_u B| = 2|eB|/3$ and $m_u = m_f$, we have the final result

$$\Gamma_{3,g}^{LLL} = \frac{g^2}{2\pi^2 m_f^2} \int_0^1 du \int_0^\infty dk_\perp\, k_\perp e^{-\frac{3k_\perp^2}{|eB|}} \frac{u}{u^2 + \gamma(1-u)} \left[1 + \frac{(2-u)u}{u^2 + \gamma(1-u)} \right]. \tag{E.55}$$

Bibliography

[1] C. Thompson and R. C. Duncan. Neutron Star Dynamos and the Origins of Pulsar Magnetism. *Astrophys. J*, 408:194, 1993.

[2] R. C. Duncan and C. Thompson. Formation of Very Strongly Magnetized Neutron Stars: Implications for Gamma-Ray Bursts. *Astrophys. J*, 392:L9, 1992.

[3] V. V. Skokov, A. Y. Illarionov, and V. D. Toneev. Estimate of the magnetic field strength in heavy-ion collisions. *Int.J.Mod.Phys.A*, 24(31):5925–5932, 2009.

[4] D. E. Kharzeev, L. D. McLerran, and H. J. Warringa. The effects of topological charge change in heavy ion collisions: "Event by event P and CP violation". *Nucl. Phys. A*, 803(3):227 – 253, 2008.

[5] Y. Hidaka and A. Yamamoto. Charged vector mesons in a strong magnetic field. *Phys. Rev. D*, 87:094502, 2013.

[6] E. V. Luschevskaya, O. E. Solovjeva, O. A. Kochetkov, and O. V. Teryaev. Magnetic polarizabilities of light mesons in SU(3) lattice gauge theory. *Nucl. Phys. B*, 898:627 – 643, 2015.

[7] A. Ayala, R. L. S. Farias, S. Hernández-Ortiz, L. A. Hernández, D. Manreza Paret, and R. Zamora. Magnetic field dependence of the neutral pion mass in the linear sigma model coupled to quarks: The weak field case. *Phys. Rev. D*, 98:114008, 2018.

[8] A. Das and N. Haque. Neutral pion mass in the linear sigma model coupled to quarks at arbitrary magnetic field. *Phys. Rev. D*, 101:074033, 2020.

[9] M. Coppola, D. Gomez Dumm, S. Noguera, and N. N. Scoccola. Neutral and charged pion properties under strong magnetic fields in the NJL model. *Phys. Rev. D*, 100:054014, 2019.

[10] J. Li, G. Cao, and L. He. Gauge invariant masses of pions in a strong magnetic field within Nambu-Jona-Lasinio model. arXiv 2009.04697, 2020.

[11] A. Ayala, J. L. Hernández, L. A. Hernández, R. L. S. Farias, and R. Zamora. Magnetic corrections to the boson self-coupling and boson-fermion coupling in the linear sigma model with quarks. *Phys. Rev. D*, 102:114038, 2020.

[12] A. Ayala, J. L. Hernández, L. A. Hernández, R. L. S. Farias, and R. Zamora. Magnetic field dependence of the neutral pion mass in the linear sigma model with quarks: The strong field case. *Phys. Rev. D*, 103(5), 2021.

[13] V. A. Miransky and I. A. Shovkovy. Quantum field theory in a magnetic field: From quantum chromodynamics to graphene and Dirac semimetals. *Phys. Rep.*, 576:1–209, 2015.

[14] N. Mikheev A. Kuznetsov. *Electroweak Processes in External Active Media*. Springer Tracts in Modern Physics 252. Springer-Verlag Berlin Heidelberg, 1 edition, 2013.

[15] V. P. Gusynin, V. A. Miransky, and I. A. Shovkovy. Theory of the magnetic catalysis of chiral symmetry breaking in QED. *Nucl. Phys. B*, 563:361–389, 1999.

[16] G. W. Semenoff, I. A. Shovkovy, and L. C. R. Wijewardhana. Universality and the magnetic catalysis of chiral symmetry breaking. *Phys. Rev. D*, 60:105024, 1999.

[17] I. A. Shovkovy. Magnetic Catalysis: A Review. *Lect. Notes Phys.*, page 13–49, 2013.

[18] G. S. Bali, F. Bruckmann, G. Endrődi, Z. Fodor, S. D. Katz, S. Krieg, A. Schäfer, and K. K. Szabó. The QCD phase diagram for external magnetic fields. *J. High Energy Phys.*, 2012(44), 2012.

[19] G. S. Bali, F. Bruckmann, G. Endrődi, Z. Fodor, S. D. Katz, and A. Schäfer. QCD quark condensate in external magnetic fields. *Phys. Rev. D*, 86:071502, 2012.

[20] G. S. Bali, F. Bruckmann, G. Endrődi, S. D. Katz, and A. Schäfer. The QCD equation of state in background magnetic fields. *J. High Energy Phys.*, 2014(177), 2014.

[21] R. L. S. Farias, K. P. Gomes, G. Krein, and M. B. Pinto. Importance of asymptotic freedom for the pseudocritical temperature in magnetized quark matter. *Phys. Rev. C*, 90:025203, 2014.

[22] M. Ferreira, P. Costa, O. Lourenço, T. Frederico, and C. Providência. Inverse magnetic catalysis in the $(2 + 1)$-flavor Nambu-Jona-Lasinio and Polyakov-Nambu-Jona-Lasinio models. *Phys. Rev. D*, 89:116011, 2014.

[23] A. Ayala, M. Loewe, and R. Zamora. Inverse magnetic catalysis in the linear sigma model with quarks. *Phys. Rev. D*, 91:016002, 2015.

[24] A. Ayala, C. A. Dominguez, L. A. Hernández, M. Loewe, and R. Zamora. Magnetized effective QCD phase diagram. *Phys. Rev. D*, 92:096011, 2015.

[25] A. Ayala, M. Loewe, A. J. Mizher, and R. Zamora. Inverse magnetic catalysis for the chiral transition induced by thermo-magnetic effects on the coupling constant. *Phys. Rev. D*, 90:036001, 2014.

[26] R. L. S. Farias, V. S. Timóteo, S. S. Avancini, M. B. Pinto, and G. Krein. Thermo-magnetic effects in quark matter: Nambu-Jona-Lasinio model constrained by lattice QCD. *Eur. Phys. J. A*, 53(101), 2017.

[27] A. Ayala, C. A. Dominguez, L. A. Hernández, M. Loewe, A. Raya, J. C. Rojas, and C. Villavicencio. Thermomagnetic properties of the strong coupling in the local Nambu-Jona-Lasinio model. *Phys. Rev. D*, 94:054019, 2016.

[28] E. J. Ferrer, V. de la Incera, and X. J. Wen. Quark Antiscreening at Strong Magnetic Field and Inverse Magnetic Catalysis. *Phys. Rev. D*, 91:054006, 2015.

[29] A. Ayala, C.A. Dominguez, L.A. Hernández, M. Loewe, and R. Zamora. Inverse magnetic catalysis from the properties of the QCD coupling in a magnetic field. *Phys. Lett. B*, 759:99 – 103, 2016.

[30] A. Ayala, J. J. Cobos-Martínez, M. Loewe, M. E. Tejeda-Yeomans, and R. Zamora. Finite temperature quark-gluon vertex with a magnetic field in the hard thermal loop approximation. *Phys. Rev. D*, 91:016007, 2015.

[31] A. Ayala, C. A. Dominguez, S. Hernández-Ortiz, L. A. Hernández, M. Loewe, D. Manreza Paret, and R. Zamora. Thermomagnetic evolution of the QCD strong coupling. *Phys. Rev. D*, 98:031501, 2018.

[32] N. Mueller, J. A. Bonnet, and C. S. Fischer. Dynamical quark mass generation in a strong external magnetic field. *Phys. Rev. D*, 89:094023, 2014.

[33] N. Mueller and J. M. Pawlowski. Magnetic catalysis and inverse magnetic catalysis in QCD. *Phys. Rev. D*, 91:116010, 2015.

[34] A. Bandyopadhyay and R. L. S. Farias. Inverse magnetic catalysis, how much do we know about?. arXiv 2003.11054, 2020.

[35] G. S. Bali, B. B. Brandt, G. Endrődi, and B. Gläßle. Weak Decay of Magnetized Pions. *Phys. Rev. Lett.*, 121:072001, 2018.

[36] Sh. Fayazbakhsh and N. Sadooghi. Weak decay constant of neutral pions in a hot and magnetized quark matter. *Phys. Rev. D*, 88:065030, 2013.

[37] Y. A. Simonov. Pion decay constants in a strong magnetic field. *Phys. At. Nucl.*, 79:455–460, 2016.

[38] R. M. Aguirre. In medium properties of K^0 and ϕ mesons under an external magnetic field. *Eur. Phys. J. A*, 55(2), 2019.

[39] T. Yoshida and K. Suzuki. Heavy meson spectroscopy under strong magnetic field. *Phys. Rev. D*, 94:074043, 2016.

[40] D. Dudal and T. G. Mertens. Melting of charmonium in a magnetic field from an effective AdS/QCD model. *Phys. Rev. D*, 91:086002, 2015.

[41] K. Marasinghe and K. Tuchin. Quarkonium dissociation in quark-gluon plasma via ionization in a magnetic field. *Phys. Rev. C*, 84:044908, 2011.

[42] P. Gubler, K. Hattori, S. H. Lee, M. Oka, S. Ozaki, and K. Suzuki. D mesons in a magnetic field. *Phys. Rev. D*, 93:054026, 2016.

[43] C. S. Machado, R. D. Matheus, S. I. Finazzo, and J. Noronha. Modification of the B meson mass in a magnetic field from QCD sum rules. *Phys. Rev. D*, 89:074027, 2014.

[44] S. Cho, K. Hattori, S. H. Lee, K. Morita, and S. Ozaki. QCD Sum Rules for Magnetically Induced Mixing between η_c and J/ψ. *Phys.Rev.Lett.*, 113:172301, 2014.

[45] S. Cho, K. Hattori, S. H. Lee, K. Morita, and S. Ozaki. Charmonium spectroscopy in strong magnetic fields by QCD sum rules: S-wave ground states. *Phys. Rev. D*, 91:045025, 2015.

[46] S. Ghosh, A. Mukherjee, M. Mandal, S. Sarkar, and P. Roy. Spectral properties of the ρ meson in a magnetic field. *Phys. Rev. D*, 94:094043, 2016.

[47] A. Bandyopadhyay and S. Mallik. Rho meson decay in the presence of a magnetic field. *Eur. Phys. J. C*, 77:771, 2017.

[48] G. S. Bali, B. B. Brandt, G. Endrődi, and B. Gläßle. Meson masses in electromagnetic fields with Wilson fermions. *Phys. Rev. D*, 97:034505, 2018.

[49] H. T. Ding, S. T. Li, A. Tomiya, X. D. Wang, and Y. Zhang. Chiral properties of $(2 + 1)$-flavor QCD in strong magnetic fields at zero temperature. arXiv 2008.00493, 2020.

[50] M. Lévy. M. Gell-Mann. The axial vector current in beta decay. *Il Nuovo Cimento*, 16:705–726, 1960.

[51] B. R. Holstein J. F. Donoghue, E. Golowich. *Dynamics of the standard model*. Cambridge University Press, 1992.

[52] J. S. Schwinger. On gauge invariance and vacuum polarization. *Phys. Rev.*, 82:664–679, 1951.

[53] A. V. Kuznetsov, A. A. Okrugin, and A. M. Shitova. Propagators of charged particles in an external magnetic field, expanded over Landau levels. *Int. J. Mod. Phys. A*, 30:1550140, 2015.

[54] A. Ayala, A. Sánchez, G. Piccinelli, and S. Sahu. Effective potential at finite temperature in a constant magnetic field: Ring diagrams in a scalar theory. *Phys. Rev. D*, 71:023004, 2005.

[55] Ashok Das. *Finite temperature field theory*. WS, 1997.

[56] A. Ayala, L. A. Hernández, A. J. Mizher, J. C. Rojas, and C. Villavicencio. Chiral transition with magnetic fields. *Phys. Rev. D*, 89:116017, 2014.

[57] A. Ayala, S. Hernández-Ortiz, and L. A. Hernández. QCD phase diagram from chiral symmetry restoration: analytic approach at high and low temperature using the linear sigma model with quarks. *Rev. Mex. de Fis.*, 64:302 – 313, 06 2018.

[58] M. E. Carrington. The effective potential at finite temperature in the Standard Model. *Phys. Rev. D*, 45:2933–2944, 1992.

[59] M. E. Peskin and D. V. Schroeder. *An introduction to quantum field theory*. Frontiers in Physics. Addison-Wesley, 1995.